AN ALGORITHM FOR OPTIMIZING PACKET SIZE

IN MOBILE AD HOC NETWORKS

By

DONG CHUL GO

Bachelor of Science

Korea Air Force Academy

Chung-Buk, Republic of Korea

1993

Submitted to the Faculty of the
Graduate College of the
Oklahoma State University
in partial fulfillment of
the requirements for
the Degree of
MASTER OF SCIENCE
July, 2005

AN ALGORITHM FOR OPTIMIZING PACKET SIZE IN

MOBILE AD HOC NETWORKS

Thesis Approved:

Jong-Moon Chung

Thesis Adviser

Gary G. Yen

Charles F. Bunting

A. Gordon Emslie

Dean of the Graduate College

ACKNOWLEDGEMENTS

My sincerely appreciation goes to the Air Force and the Air Force Academy of the Republic of Korea. The training and education of these organizations have gave me the confidence, pride, and honor to live a righteous life, and have taught me precious ethics of integrity and diligence, which serve as a guide to my daily life.

I wish to express my deepest appreciation to my thesis advisor Dr. Jong-Moon Chung for his guidance on my thesis and his encouragements. A rigorous scientist and a hard working engineer, Dr. Chung made the progress of my thesis both inspiring and interesting. My sincere thanks also go to my other committee members Dr. Gary G. Yen and Dr. Charles F. Bunting for their technical advice and helpful reviews of my thesis. I also wish to thank Dr. Soo Yong Choi for his help on the channel modeling and also in regards to the class lectures which were helpful. I am also grateful to my colleagues of the ACSEL & OCLNB laboratories of the Oklahoma State University for their kind help and friendship.

Most of all I would like to thank my parents for their love and guidance, which has lead me to whom I am today, and also to my wife Su Young Lee and son Myung-Jin for their love, support, and patience. It is my family's love that encourages me to study hard and leads me to happiness.

TABLE OF CONTENTS

Chapter Page

I. Introduction 1

II. System Model 5

2.1 Overview 5
2.2 Transmission Model 5
2.3 Channel Model 6
2.4 Packet Reception Model 8

III. Mobility Model 13

3.1 Overview 13
3.2 Gauss-Markov Mobility Model 13

IV. Multiple Access Technologies 18

4.1 Overview 18
4.2 Slotted ALOHA Network 19
4.3 CSMA 21
4.4 CSMA/CD 22
4.5 CSMA/CA 23

V. Derivation of the BER Distribution for MANET Nodes 25

5.1 Overview 25
5.2 The Distribution of Link Distance 25
5.3 The Distribution of the SINR 30
5.4 The Distribution of the BER 33

VI. Derivation and Experimentation of the MANET Efficiency Applying the Mobility Model 37

6.1 The Optimal Packet Size 37
6.2 Analysis of the Protocol Efficiency 40

VII. Conclusion 57

References 59

Appendix : Mathematical Derivation 61

1. Proof of (2-8) 61
2. Proof of (2-11) 62
3. Proof of (2-13) 63
4. Proof of (5-11) 64
5. Proof of (5-14) 65
6. Proof of (5-17) 66
7. Proof of (5-20) 67

LIST OF TABLES

Table Page

Table 2-1: The values of path loss exponent. 7
Table 3-1: Parameter values for Gauss-Markov mobility model..... 17
Table 5-1: Parameter values for estimation of the distribution of BER. 31
Table 6-1: Default parameter values of the Qualnet simulator. 45
Table 6-2: Parameter values for the simulation. 47
Table 6-3: The performance gain obtainable from the algorithm proposed in this thesis. 56

LIST OF FIGURES

Figure Page

Figure 3-1: The mobility pattern of the Gauss-Markov model [9]. 16
Figure 5-1: Randomly distributed mobile nodes. 26
Figure 5-2: The PDF of the link distance..... 29
Figure 5-3: The PDF and CDF of the SINR. 32
Figure 5-4: The conversion map of the SINR to BER. 33
Figure 5-5: The error ratio of approximation DPSK equation based on Figure 5-4. 34
Figure 5-6: The PDF of BER. 36
Figure 6-1: The throughput and optimal packet size for a given p. 39
Figure 6-2: The efficiency for a given Q. 44
Figure 6-3: Packet format of the sublayers. 46
Figure 6-4: The average efficiency (k_{pre} = 544 bytes). 48
Figure 6-5: The average efficiency (k_{pre} = 32 bytes). 49
Figure 6-6: The average efficiency (k_{pre} = 2312 bytes). 50
Figure 6-7: The efficiency ratio (k_{pre} = 544 bytes). 51
Figure 6-8: The efficiency ratio (k_{pre} = 32 bytes). 52
Figure 6-9: The efficiency ratio (k_{pre} = 2312 bytes). 53
Figure 6-10: The average efficiency ratio. 55

NOMENCLATURE

ACK	Acknowledgement
ADCF	Adaptive IEEE 802.11 Distributed Coordination Function
ARQ	Automatic Repeat reQuest
AQOR	Ad hoc QoS On-demand Routing
BER	Bit Error Rate
CEDAR	Core-Extraction Distributed Ad hoc Routing
CDF	Cumulative Distribution function
CRC	Cyclic Redundancy Check
CSMA	Carrier Sensing Multiple Access
CSMA/CA	Carrier Sensing Multiple Access/Collision Avoidance
CSMA/CD	Carrier Sensing Multiple Access/Collision Detection
CTS	Clear To Send
DCF	Distributed Coordination Function
DiffServ	Differentiated Service
DPSK	Differential Phase Shift Keying
FCS	Frame Sequence Check
FQMM	Flexible QoS Model for Mobile Ad Hoc Network
IP	Internet Protocol
LAN	Local Area Network

MAC	Medium Access Control
MANET	Mobile Ad Hoc Network
PCS	Personal Communication System
PDF	Probability Density Function
PMF	Probability Mass Function
QoS	Quality of Service
RTS	Request To Send
SINR	Signal to Interference plus Noise Ratio
TDM	Time Division Multiplexing
UDP	User Datagram Protocol
WLAN	Wireless Local Area Network

Chapter 1

Introduction

A mobile ad hoc network (MANET) consists of a set of mobile users that communicate with each other over a mobile wireless channel. In a MANET the nodes are assumed to be free to move and a mobile node becomes potentially a router to dynamically establish routes without the aid of a fixed infrastructure or centralized management. MANET is a self-organizing and self-configuring multi-hop wireless network. Ad hoc networks were initially proposed for military applications such as battle field communication and disaster recovery. Quality of service (QoS) in MANETs was developed based on commercial interest and multimedia technology for the purpose of user satisfaction and efficient network resource utilization. QoS in wire-based networks have been well developed with several techniques, over provisioning of resources, network traffic engineering, and differentiated services (DiffServ). However, the techniques used in wire-based networks can’t be directly adapted to MANETs because of the constraints in MANETs, such as, poor bandwidth resources in wireless communications, the dynamic topology in ad hoc networks, and the limited storing capability and power capability of mobile nodes. In the Transport Control Protocol (TCP)/Internet Protocol (IP) or Open Systems Interconnection (OSI) 7 layer network architecture, each layer was developed

independently to guarantee that one layer can be developed relatively independent to other layers. For example, the software in the application layer can be easily changed relatively independent to the implementation of the other layers'. This approach provides a convenience in improving each layer but result in poor efficiency in using network resources due to the extra overhead that each layer adds on. There is a trade-off between convenience and efficiency. Various QoS models and protocols have been proposed to improved the QoS in MANETs, for example, the flexible QoS model for MANET (FQMM) [1], ISIGNIA [2] for QoS signaling, the core-extraction distributed ad hoc routing algorithm (CEDAR) [3], ad hoc QoS on-demand routing (AQOR) [4], and the IEEE 802.11 DCF scheme (ADCF) [5] for QoS in MAC layer for wireless local area networks (WLANs).

The high efficiency is an essential requirement for QoS in MANETs due to the constraints of battery power and limited channel stability. In [15] it has been revealed that the recent research trends in MANET research has result in over 1,300 MANET related papers in IEEE/IEE Electronic Library (IEL online) from 1998 to 2003 and fifteen major MANET issues from various aspects are introduced: routing, multicasting, broadcasting, location service, clustering, mobility management, TCP/UDP, IP addressing, multiple access, radio interference, bandwidth management, power management, security, fault tolerance, QoS/multimedia, and standards/products. Compare to the total number of number of papers, the number of papers focusing on mobility, IP address, and fault tolerance combined are less than 100, which shows a relative smaller interest in an important research area [15]. One of the generic problems in MANETs is the mobility.

The network topology and link status change dramatically due to mobility and these changes cause most of the technical issues in MANETs.

In this thesis we focus on the effect of mobility on the performance. In [13], the network capacity of wireless ad hoc networks was studied and the boundary capacity was obtained for non-mobile ad hoc networks. A standard measurement of mobility was proposed in [17] for evaluating MANET performance and the remoteness obtained from a Gamma probability density function (PDF) is compared with the link change rate obtained from simulation. In MANETs, the channel status changes unpredictably mainly due to mobility and also due to other wireless channel characteristics such as multi-path fading, shadowing by obstacles, and interference from other users. In wireless networks, the packet size affects the performance of the protocol due to the high error rate and time variation of mobile wireless channels. In [6] an algorithm that optimizes the packet size without requiring *a priori* information of the channel conditions has been developed. The channel status is estimated from the number of retransmission requests and the packet size to maximize the throughput performance is chosen based on the estimated channel condition. In [6] the channel condition is estimated with the assumption of an uniform distribution of the bit error rate (BER).

In this thesis, the algorithm of [6] is extended with the non-uniform distribution of the BER. In this thesis the packet size is adapted to maximize the communication performance through the automatic repeat request (ARQ) protocol. The optimal packet size is chosen by an algorithm based on the estimation of the channel from the number of

retransmission requests and the link statistics obtained from the mobility pattern. By adapting the distribution of the BER obtained from the mobility apttern analysis, it is possible to estimate more accurate channel conditions from the number of retransmission requests and to improve the overall system performance. In Chapter 3, the distribution of the BER based on the Gauss-Markov mobility model for IEEE 802.11 wireless local area networks (WLANs) is obtained. This algorithm can be combined with other protocols to improve the QoS in MANETs. Also the statistics obtained from the mobility pattern can be used for optimization of other protocols.

There are seven chapters in this thesis. Chapter 2 describes the system model where the transmission model, channel model, and packet reception model are explained. Chapter 3 explains the detailed implementation of the Gauss-Markov mobility model used in the simulation. Chapter 4 focuses on multiple access techniques and their performance. Chapter 5 introduces the distribution of the BER adapted the Gauss-Markov mobility model on a circular shape wireless network region. Chapter 6 compares the efficiency of optimal packet sizes and the efficiency of an algorithm that chooses a packet size to maximize the performance. Chapter 7 presents the conclusions and discusses future work.

Chapter 2

System Model

2.1 Overview

The mobile ad hoc network model to be applied in the following mathematical derivations consists of N mobile nodes which are randomly distributed with a uniform PDF in a circular area of radius is R. Let $n_i(t)$ be the location of node i at time t. It is assumed that the process $\{n_i(\cdot)\}$ is stationary and ergodic and all the nodes are independent and identically distributed (i.i.d.).

2.2 Transmission Model

For the transmission model, let $G(t)$ be the transmission group including all the nodes which transmit signals at time t and $N_G(t)$ be the number of nodes in the transmission group at time t. It is assumed that the process $\{G(\cdot)\}$ is stationary and the average of $N_G(t)$ is a fixed value denoted as N_G. Then the average of the group density ($U(t)$) is

also constant ($\overline{U}$), where the group density is the ratio of the number of active nodes in the transmission group to the total number of nodes in the network.

$$E[U(t)] = E\left[\frac{N_G(t)}{N}\right] = \frac{N_G}{N} = \overline{U}\,. \tag{2-1}$$

Let $P_i(t)$ be the transmission power of node *i* at time *t*. It is assumed that all nodes use a common power level, $\overline{P}$, and do not change the transmission power. The transmission power of node *i* is zero when node *i* is not a member of a transmission group at time *t*. This is based on the assumption that members of different transmission groups will be using different non-interfering frequencies, time-divisions, or code-divisions. The transmission power can be represented as

$$P_i(t) = \begin{cases} \overline{P}, & i \in G(t) \\ 0, & i \notin G(t) \end{cases}. \tag{2-2}$$

2.3 Channel Model

Let $D_{ij}(t) = |n_i(t) - n_j(t)|$ represent the link distance between node *i* and node *j* and $\phi_{ij}(t, D_{ij}(t))$ be the channel gain. The path-loss power law model is assumed for radio model so the received power is reduced with link distance. The received power at node *j* from node *i* at time *t* is $P_i(t)\phi_{ij}(t, D_{ij}(t))$, where the channel gain is $\eta_0 \eta_{ij}^{tx}(t)\eta_{ij}^{rx}(t)[D_{ij}(t)]^{-\alpha_{ij}(t)}$. In the model applied in this research, it is assumed that the channel is stationary and ergodic so that the channel gain depends only on the link

distances, which means the transmitting and receiving gain ($\eta_{ij}^{tx}(t)\eta_{ij}^{rx}(t)$) are constant with time and links, η_0 is the gain of the receiver's automatic gain controller (AGC), and the power decaying parameter is also constant $\alpha_{ij}(t)=\alpha$. The channel gain becomes

$$\phi_{ij}\left(t, D_{ij}(t)\right) = C_0 D_{ij}(t)^{-\alpha}. \tag{2-3}$$

From (2-3), considering the assumptions made we simplify the equation such that the channel gain depends only on the link distance. Therefore it is assumed that $\eta_0\eta_{ij}^{tx}(t)\eta_{ij}^{rx}(t)=1$ for convenience of the analysis. So the received power at node j from node i at time t ($S\left(D_{ij}(t)\right)$) can be written as

$$P_{RX}\left(D_{ij}(t)\right) = \begin{cases} \dfrac{\overline{P}}{D_{ij}(t)^{\alpha}}, & i \in G(t) \\ 0, & i \notin G(t) \end{cases}. \tag{2-4}$$

Appropriate values of α depends on the wireless environment and the application of the wireless system. In [18] a range of α values based on application and environment are presented and summarized here in Table 2-1.

Table 2-1: The values of path loss exponent.

Wireless environment	**Path loss exponent, α**
Free space	2
In building (obstructed)	4 ~ 6
Shadowed urban area	3 ~ 5
Urban area	2.7 ~ 3.5

2.4 Packet Reception Model

The signal to interference plus noise ratio (SINR) of the signal from node i to node j at time t [13] is

$$X\left(D_{ij}(t)\right)=\frac{\overline{P}D_{ij}(t)^{-\alpha}}{\rho N_0 W+\overline{P}\sum_{\substack{n\in G(t)\\ n\neq i}} D_{nj}(t)^{-\alpha}} \tag{2-5}$$

where ρ is the noise factor, N_0 is the thermal noise, and W is the common bandwidth of the signal from node i to node j at time t. Let $I_{ij}(t)$ be the interference of the link from node i to node j. The interference of the link can be express as

$$I_{ij}(t)=\overline{P}\sum_{\substack{n\in G(t)\\ n\neq i}} D_{nj}(t)^{-\alpha}\ . \tag{2-6}$$

The mean conditional SINR becomes

$$E\left[X\left(D_{ij}(t)\right)\right]=\frac{\overline{P}D_{ij}{}^{-\alpha}}{\rho N_0 W+E\left[\overline{P}\sum_{\substack{n\in G(t)\\ n\neq i}} D_{nj}(t)^{-\alpha}\right]} \tag{2-7}$$

where D denotes the distance random variable. It is assumed that the source node is a member of the transmission group ($G(t)$) and the destination node receives a signal from the source node at a link distance $D_{ij}(t)$ at time t. Let $f_D\left(D_{ij}(t)\right)$ be the probability density function (PDF) of the link distance. Based on the assumptions, the link distance from the other nodes (except the source to the destination node) are independent and

identically distributed (i.i.d.). So each link has the same probability distribution as the others and all links are mutually independent. Considering the ergodic channel assumption, the mean interference can be written as,

$$I_0 = E\left[\overline{P}\sum_{\substack{n\in G(t)\\ n\neq i}} D_{nj}(t)^{-\alpha}\right] = \overline{P}(N_G - 1)\int_0^\infty D_{ij}^{-\alpha} f_D(D_{ij})dD_{ij}\ . \tag{2-8}$$

The derivation of (2-8) is included in the Appendix. Then the mean conditional SINR can be written as

$$E\left[X(D_{ij}(t))\right] = \frac{\overline{P}D_{ij}^{-\alpha}}{\rho N_0 W + I_0}\ . \tag{2-9}$$

If the PDF of the link distance is known, the mean conditional SINR can be obtained from (2-9).

After the channel is sensed at node *j*, the signal from node i to node *j* is decoded at node *j*. At time *t*, node *j* can sense the channel if

$$\left[\rho N_0 W + E\left[\overline{P}\sum_{n\in G(t)} D_{nj}(t)^{-\alpha}\right]\right] \geq P_{sen} \tag{2-10}$$

where P_{sen} is the receive sensitivity which is the minimum power required for the carrier sensing system to detect a signal. From (2-9) and (2-10) the mean carrier sensing range is

$$R_{sen} = \begin{cases} \left[\dfrac{\overline{P}}{P_{sen} - \rho N_0 W - I_0} \right]^{\frac{1}{\alpha}}, & P_{sen} \geq \left(I_0 + \rho N_0 W \right) \\ \infty \qquad\qquad , & P_{sen} < \left(I_0 + \rho N_0 W \right). \end{cases} \tag{2-11}$$

The derivation of (2-11) is included in the Appendix. The range represented by R_{sen} does not mean that communication can be necessarily established, it only indicates the range that the minimum receiver sensitivity is satisfied. In reality, the communication range is determined by various system parameters such as the transmission power, channel gain, noise factor, and required signal-to-noise ratio. There are two packet reception models. One is the SINR threshold based model [13] that decides successful reception of a packet based on a comparison to the minimum SINR. In this model, the signal from node *i* to node *j* is received without error and all packets are accepted successfully if

$$\frac{\overline{P} D_{ij}(t)^{-\alpha}}{\rho N_0 W + \overline{P} \sum\limits_{\substack{n \in G(t) \\ n \neq i}} D_{nj}(t)^{-\alpha}} \geq \gamma_{\min} \tag{2-12}$$

where $\gamma_{\min}$ is the minimum SINR requirement for successful communication. From (2-9) and (2-12) the maximum average communication range of the SINR threshold based model is

$$R_{\max} = \left(\frac{\overline{P}}{\gamma_{\min} \left(\rho N_0 W + I_0 \right)} \right)^{\frac{1}{\alpha}}. \tag{2-13}$$

The derivation of (2-13) is included in the Appendix. The other packet reception model is based on the BER that decides the successful reception of a packet based on the BER. We

define $H(\cdot)$ as the function that converts the SINR to the BER and $\mathrm{B}_{ij}(t)$ as the BER of the signal from node *i* to node *j* at time *t*. Then the BER of the signal from node *i* to node *j* can be represented as,

$$\mathrm{B}_{ij}(t) = H\left(E\left[X\left(D_{ij}(t)\right)\right]\right). \tag{2-14}$$

The calculation of the BER from the SINR is complex and there is no exact equation that defines the conversion. Therefore the mapping functions are used to convert SINR to BER based on the Qualnet simulator [12] and an approximated equation will be induced in Chapter 5. The packet error rate is calculated from the BER, packet size, and error control coding. The packet reception model based on the SINR can not provide the packet error rate of the variable channel condition caused by the mobility. It can only provide the successful link establishment based on the SINR requirement. In this thesis, the BER based packet reception model will be adapted for the algorithm in MANET. The average communication range of the BER based model where the BER value p can be obtained from

$$R_{com}(p) = \left(\frac{\overline{P}}{H^{(-1)}(p)\left(\rho N_0 W + I_0\right)}\right)^{\frac{1}{\alpha}} \tag{2-15}$$

where $H^{(-1)}(\cdot)$ represents the inverse function of $H(\cdot)$. This analysis is focused above the physical layer where packet data can be processed. Packet error rate is influence by the BER, packet sizes, and error control coding scheme. Let *k* be the size of payload bits and *h* be the size of header bits. Then the packet error rate for a given value of BER (p) is

$$P_E = 1 - \sum_{i=0}^{c} \binom{k+h}{i} p^i (1-p)^{k+h-i} \tag{2-16}$$

where c is the number of correctable bits by error control coding. This thesis assumes the use of optimal automatic repeat-request (ARQ) protocol in that only packets containing errors are retransmitted. We define κ as the packet failure probability in which a packet fails to be received properly despite applying a maximum Ω trials of retransmission (i.e., the retransmission limit) and an error control decoder with the capability to correct up to c errors per fixed length packet. Based on this definition κ can be represented as

$$\kappa = 1 - (1 - P_E) \sum_{j=0}^{\Omega} (P_E)^j = (P_E)^{\Omega+1}. \tag{2-16}$$

For example, the IEEE 802.11b MAC protocol [14] has a retransmission limit of 4 for long packets and 7 for short packets.

Chapter 3

Mobility Model

3.1 Overview

In this chapter, the Gauss–Markov mobility model is adapted to characterize mobile nodes in a MANET environment. In [7], the Gauss-Markov mobility model was applied to the analysis of mobility management of Personal Communication System (PCS) mobile communication networks which will be extended here in this chapter's analysis for MANETs.

3.2 Gauss-Markov Mobility Model

In the Gauss-Markov mobility model, a mobile node's velocity is assumed to be correlated in time and characterized as a stationary Gauss-Markov process. The autocorrelation function of a stationary Gauss-Markov process with variance $E[v(t)] = \sigma^2$ and time constant $T_0 = f_o^{-1}$ is,

$$R_v(\tau) = E[v(t)v(t+\tau)] = \sigma^2 e^{-f_0|\tau|} \tag{3-1}$$

where f_0^{-1} represents the degree of memory in the mobility pattern. For the discrete process, if Δt denotes the time interval of sampling, then $v_n = v(n\Delta t)$. The discrete representation of the autocorrelation function is

$$R_v(k) = E[v_n v_{n+k}] = \sigma^2 e^{-f_0|k\Delta t|}. \tag{3-2}$$

Let the tuning parameter be $\varphi = e^{-f_0 \Delta t}$. Then the discrete representation of (3-1) can be written as [8]

$$v_n = \varphi v_{n-1} + (1-\varphi)\mu_v + \sqrt{(1-\varphi^2)}G_{n-1}^v. \tag{3-3}$$

Similarly, the direction of the mobile node can be defined to be the same form as (3-3) [9].

$$d_n = \varphi d_{n-1} + (1-\varphi)\mu_d + \sqrt{(1-\varphi^2)}G_{n-1}^d \tag{3-4}$$

where μ_v and μ_d are the mean values of the speed and direction as $n \to \infty$. In addition, G_n^v and G_n^d are independent, uncorrelated, and stationary Gaussian processes, with zero means and standard deviations $\sigma_v{}^2 = \sigma_d{}^2 = \text{var}[v_n]$ as $n \to \infty$. Brownian motion can be obtained when $\varphi = 0$ and linear motion can be obtained when $\varphi = 1$. Brownian motion is a totally random and memoryless motion and hence the time constant is zero, which makes the value of φ be zero. The time constant of linear motion is infinite, which makes $\varphi = 1$. The intermediate values of φ can be obtained from the time constant T_0. Based on this, the tuning parameter can be represented as,

$$\varphi = e^{-\Delta t / T_0} \tag{3-5}$$

where Δt^{-1} is the sampling frequency of the discrete mobility model and $0 \le \varphi \le 1$. By setting the tuning parameter (φ) to an appropriate value, it is possible to design various mobility models. From (3-3) and (3-4), the next location is updated based on the current location, speed and direction of movement [9], as given in (3-6)

$$\begin{aligned} x_{n+1} &= x_n + v_n \cos(d_n) \\ y_{n+1} &= y_n + v_n \sin(d_n) \end{aligned} \tag{3-6}$$

where (x_{n+1}, y_{n+1}) and (x_n, y_n) are the mobile node positions at the n^{th} and $(n+1)^{th}$ time interval [9]. If the size of the network is limited and the mobile node has to remain in the network, the mobile nodes must be forced away from the edge of the network area. This can be done by changing the mean of G_n^d so that the directions of the mobile nodes are changed toward the center of the network when the mobile nodes are located outside of the network.

The network is designed as a circle with a diameter of 200 m and the initial position of the mobile node is the center of the network (100, 100) and moves for 500 seconds. The mean speed (μ_v) is fixed at 5 m/sec but the mean direction (μ_d) is initially set to zero but then changed towards the center point of the network when the nodes are located outside of the network area. The Gauss-Markov mobility model can remove the abrupt change in the position of the mobile node by adapting the time correlation model in the mobility pattern.

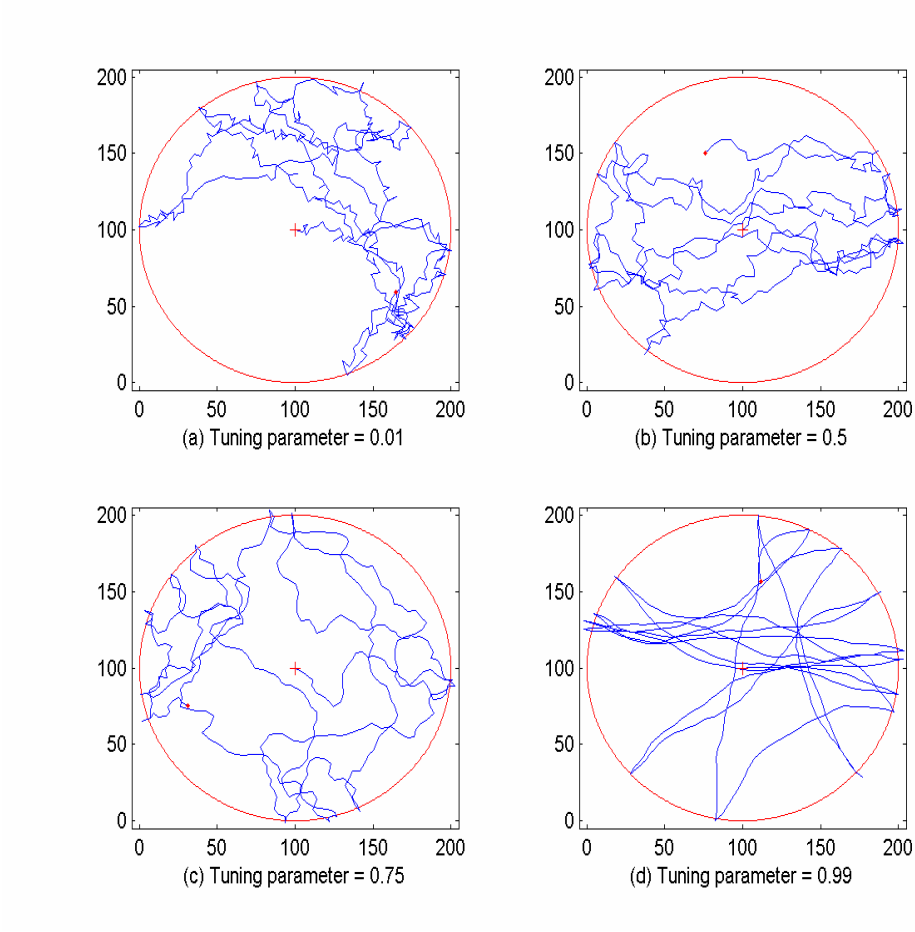

Figure 3-1: The mobility pattern of the Gauss-Markov model [9].

Figure 3-1 illustrates four examples of the traveling patterns of the Gauss-Markov mobility model by taking the parameter values shown in Table 3-1. The plus marks are the start points and the dot marks are the end points of the travel. The graphs in Figure 3-1 show that when the value of the tuning parameter (φ) is near zero, the mobility pattern follows Brownian motion, and when the value of the tuning parameter (φ) is near one, the mobility pattern is as same as that of linear movement. It is possible to generate the desired mobility patterns by changing the value of the tuning parameter (φ).

Table 3-1: Parameter values for Gauss-Markov mobility model.

Parameters	**Values**	**Parameters**	**Values**
Tuning parameters (φ)	0.01, 0.5, 0.75, 0.99	Initial position (x_0, y_0)	(100, 100)
Simulation time (T)	500 sec	Mean of G_n^v	0
Network radius (R)	100 m	Variation of G_n^v	1
Mean speed (μ_v)	5 m/s	Mean of G_n^d	0
Mean direction (μ_d)	0 (initial value)	Variation of G_n^d	1
Sampling interval (Δt)	1 sec		

Chapter 4

Multiple Access Technologies

4.1 Overview

MANETs require self-organizing and dynamic multihop wireless networking technologies, which commonly use shared wireless channels. In a shared wireless channel, which is a type of multiaccess media, the received signal is the sum of the attenuated transmitted signals from a set of other nodes, affected by fading, shadowing, delay, and noise. The method of how users can effectively share a common wireless channel to obtain a desired performance requires research in interference reduction. This allocation issue is usually done at the Medium Access Control (MAC) layer. There are two extremes among the many strategies to solve this allocation issue. One is the “free-for-all” approach where nodes transmit a signal immediately whenever a request for transmission is made. The problem of the free-for-all approach is in deciding the retransmission of the packets after collision. In this approach the collision of packets is unavoidable and so the problem of collision is solved after collision. The free-for-all approach is simple and robust but its collision probability is high and the performance deteriorates rapidly as the numbers of users increase. The other extreme is the “perfect

schedule” approach where nodes transmit a signal according to some order. The problem of collision is solved before transmitting a packet. The perfect schedule approach needs a core-system to arrange the order. When the traffic utilization rate is low the probability of collision in the free-for-all approach is small so that the system performance is degraded little by the collision of packets. Due to the advantages of its low complexity and robustness, the free-for-all approach is suitable for low user density areas. The latter approach is suitable for high density environments where the density of users is high, but a drawback of the perfect schedule approach is its high complexity and the need for a core-system (i.e., access point or base station) to arrange the order. MANETs have no infrastructure or core-system, therefore the perfect-schedule approach is not suitable as a media access control (MAC) protocol for MANETs. Therefore, we focus on the free-for-all approach and describe some possible multiple access options.

4.2 Slotted ALOHA Network

The ALOHA network was developed for radio data communication between the islands of Hawaii. The basic algorithm of the ALOHA network is that the source node sends a packet whenever a packet transmission request is made. The transmission node finds out whether the transmission was successful or a failure (i.e., experienced a collision) by listening to the broadcast from the destination node. Then if a collision occurs, the source node waits a random time and retransmits the packet. In [10] the analysis of ALOHA networks are well explained, where the idealized slotted multi-access model of [10] is studied in this section. The assumptions of the model include slotted time system,

Poisson arrivals (λ), collision or perfect reception, immediate feedback of perfect reception, no reception or error, unlimited retransmission, and no buffering. Let Θ be the throughput which is the ratio of the expected number of successful transmissions in a slot to the expected number of attempted transmissions in a slot. Let the attempted rate $\Lambda(n)$ be the expected retransmissions in a slot when the system has *n* backlogged nodes. Based on [10] the attempted rate is

$$\Lambda(n) = (m-n)q_a + nq_r \tag{4-1}$$

where m is the total number of nodes, n is the number of backlogged nodes, q_a is the probability that an unbacklogged node transmits a packet in the given slot, and q_r is the probability that a backlogged node transmits a packet in the given slot. From the above assumption, arrivals are Poisson distributed with mean λ/m, and the probability of no arrivals is $e^{-\lambda/m}$. If an unbacklogged node receives an arrival, it transmits a packet immediately. So, $q_a = 1 - e^{-\lambda/m}$. The fixed value of q_r depends on the protocol's option. The throughput of slotted ALOHA when the system has *n* backlogged nodes is

$$\Theta(n) = \Lambda(n)e^{-\Lambda(n)} \tag{4-2a}$$

and the throughput of pure ALOHA when the system has *n* backlogged nodes becomes

$$\Theta(n) = \Lambda(n)e^{-2\Lambda(n)}. \tag{4-2b}$$

The maximum throughput of pure ALOHA is $1/2e$=0.184 and that of slotted ALOHA is $\frac{1}{e} = 0.386$. Slotted ALOHA gives better performance than the pure ALOHA by reducing

the probability of collision. Slotted ALOHA can transmit packets immediately after a new packet arrives with occasional collisions. If the probability of collision is small, delay is very small, whereas time division multiplexing (TDM) techniques help avoid collisions at the expense of large delays. Pure ALOHA can send variable length packets, whereas slotted ALOHA can send only packets limited to the slot size. The maximum throughput can be obtained in ALOHA networks when the transmission rate is one. An ALOHA network is simple and easy to implement, so if the arrival rate is small, it gives a good throughput and delay performance. But if the arrival rate is high, the system becomes unstable and it gives a poor performance of throughput and delay.

4.3 CSMA

Carrier sensing multiple access (CSMA) is one of the free-for-all approaches in which nodes are prohibited from transmitting a packet when the channel is sensed to be busy. In ALOHA, nodes decide to transmit independently and so nodes do not pay attention whether other nodes are transmitting and nodes do not stop transmitting when other nodes are transmitting. However CSMA reduces the probability of collision by transmitting a packet only when the channel is sensed to be idle, so it improves the performance by utilizing the idle periods. It is possible to employ various types of node behavior when the channel is busy. There are two types of CSMA schemes according to the carrier sensing methods. In non-persistent CSMA, if the system senses the transmission channel to be busy, it waits an entire back-off period before sensing the channel again and then if it senses an idle channel, it transmits a packet immediately.

Whereas in persistent CSMA the system senses the channel again immediately after the sensing of a busy channel and then if it senses an idle channel, it transmits a packet with some probability (1 or *p*). The performance of CSMA slotted ALOHA critically depends on the ratio (β) of the propagation delay to the packet transmission time [10]. Let β be the propagation and detection delay in the packet transmission unit. Then β can be obtained from

$$\beta = \tau \frac{C}{L} \tag{4-3}$$

where τ is the time required for all nodes to detect an idle channel after a transmission ends, C is the raw channel bit rate, and L is the expected number of bits in a data packet. The maximum performance of CSMA slotted ALOHA [10] is $\frac{1}{1+\sqrt{2\beta}}$ at the point when the expected number of transmissions is $\sqrt{2\beta}$.

4.4 CSMA/CD

CDMA/collision detection (CD) is an advanced approach of CSMA in which the network protocol stops sending packets when the channel is sensed to be busy during transmission. It can improve the performance by reducing the duration of collision but it needs to sense the channel as well as send a packet at the same time. After collision, nodes back-off for a random time and sense the channel condition and if the channel is sensed to be idle, it retries to retransmit the packet. Collision occurs only when a node senses the channel is idle and transmits a packet but the other nodes also transmit a packet. This vulnerable

period is only during the propagation delay. Therefore, the performance of CSMA/CD depends on the propagation and detection delay (β). To get a bound on the throughput (Θ), the bounds of all relevant parameters are assumed according to [10] (i.e., an ideal channel, maximum propagation delay, and Poisson arrival). Then the throughput of CDMA/CD is lower bound by

$$\Theta > \frac{e^{-\beta\Lambda}}{\beta + 1/\Lambda + 2\beta\left(1 - e^{-\beta\Lambda}\right) + e^{-\beta\Lambda}}. \tag{4-4}$$

CSMA/CD is a wildly used technique for local area networks called Ethernet, which is the IEEE 802.3 protocol. In a shared wireless channel, CSMA/CD has problems of hidden nodes and exposed node.

4.5 CSMA/CA

CSMA/collision avoidance (CA) has been developed to combat the problems of the CSMA/CD hidden/exposed nodes. CSMA/CA reserves a wireless channel by using a request-to-send (RTS) message and a destination node gives clearance by using a clear-to-send (CTS) message. When the channel is sensed to be idle and communication is needed, the source node sends a RTS frame to the destination node for reservation of the channel. The destination node receiving a RTS frame sends back a CTS frame, after which the data packet is transmitted by a source node and a destination node sends back an acknowledgement (ACK) frame. Collision may occur only on RTS frames. When a source node does not receive back CTS frames from a destination node, the collision of RTS frames is detected. CSMA/CA increases the system performance by reducing the

period of collision when data packets are transmitted. To combat the hidden/exposed node problems, the nodes which listen to the CTS frame will keep quiet until it hears an ACK message from a destination node.

The mean collision period depends on the collision resolution technique after collision. The IEEE 802.11 distributed coordination function (DCF) uses an exponential back-off scheme for collision resolution, where the performance of the IEEE 802.11 DCF has been well studied in [11]. In [11], the ideal channel condition is assumed for the analysis, which means that packets are assumed errorless if there is no collision. When the number of nodes is finite, the throughput of 802.11 DCF [11] is

$$\Theta = \frac{P_{tr} P_S E[k]}{(1 - P_{tr})\sigma + P_{tr} P_S T_S + P_{tr}(1 - P_S) T_C} \tag{4-5}$$

where $E[k]$ is the average packet payload size, P_{tr} is the probability that there is at least one transmission in the considered slot times, and P_S is the probability that a transmission occurring on the channel is successful. T_C is the average time the channel is sensed busy by each station during collision, T_S is the mean time of the busy channel due to successful transmission, and σ is the duration of an empty slot time. The IEEE 802.11 DCF adapted CSMA/CA is suitable for a shared wireless channel. However the result of [16] shows that the performance of IEEE 802.11 is not satisfactory in MANETs due to several problem, which include the hidden/exposed node problems existing in multihop wireless ad hoc networks, interfering and carrier sensing range which are more than two times the size of the communication range, and the fairness problem caused by the binary exponential back-off scheme.

Chapter 5

Derivation of the BER Distribution for MANET Nodes

5.1 Overview

In MANETs, packets are forwarded from the source to the destination via multi-hop paths and the reliability of multi-hop communication paths is related to the reliability of the individual link. In chapter 2, it was assumed that the channel status is changed by only link distance, which depends on the mobility. Evidently the statistics of link distance in MANETs is an important factor. In this chapter, the distribution of the link distance between two mobile nodes which are randomly positioned in a MANET is found and the distribution of the BER is calculated.

5.2 The Distribution of Link Distance

Let the mobile nodes be randomly distributed with a uniform PDF within a circle having radius R as illustrated Figure 5-1.

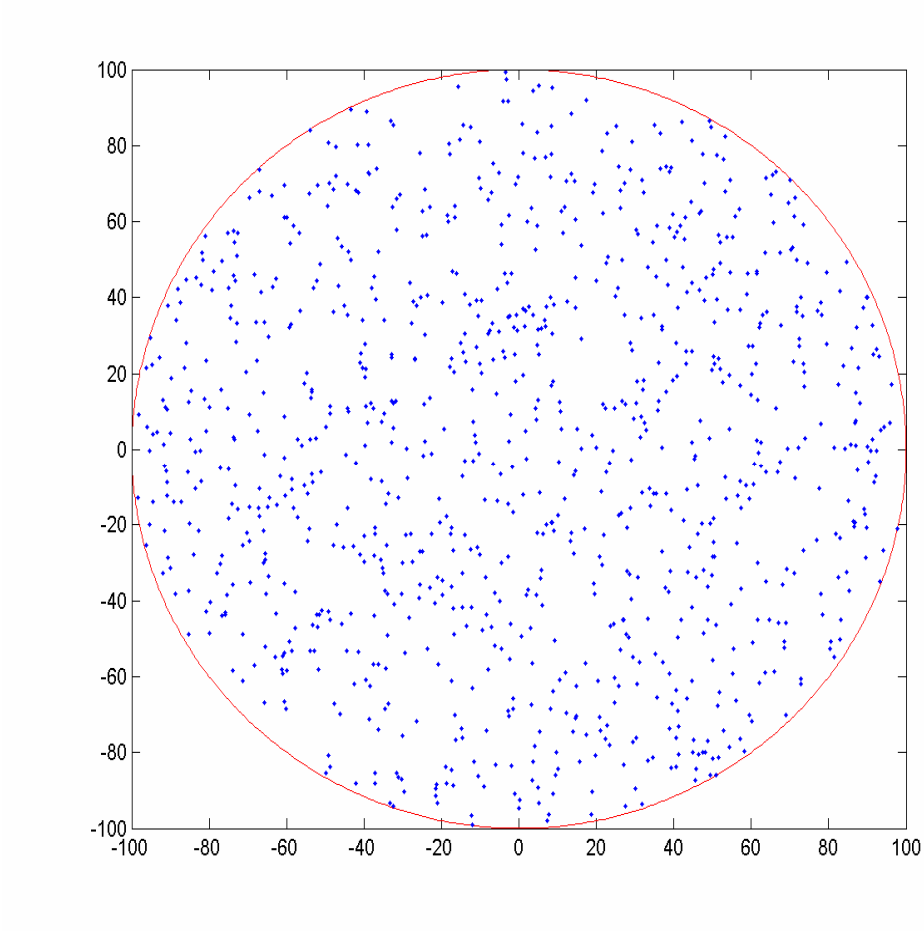

Figure 5-1: Randomly distributed mobile nodes.

The mobile nodes move according to the Gauss-Markov mobility model with the tuning parameter $\varphi = 0.71655$. Recall $n_i(t), \quad i = 1, 2, \text{K}, N$, represents the location of node *i* at time *t* and $D_{ij}(t) = |n_i(t) - n_j(t)|$ represents the distance from node *i* to node *j* at time *t*. Let *T* be the total travel time that the mobile node moves according to the Gauss-Markov mobility model. The probability that the link distance D_{ij} is less than some value *r* can be defined as

$$P\left\{D_{ij} \le r\right\} = F_{D_{ij}}\left(r\right) = \frac{1}{T}\int_0^T \mu\left(r - D_{ij}\left(t\right)\right)dt \tag{5-1}$$

where $\mu[\cdot]$ is the unit step function and $F_{D_{ij}}(\cdot)$ is the cumulative probability distribution function (CDF) of the link distance random variable between node *i* and node *j*. The mean CDF of the link distance ($F_D(r)$) is defined as

$$F_D\left(r\right) = \frac{1}{N\left(N-1\right)}\sum_{i=1}^{N}\sum_{\substack{j=1 \\ j\neq i}}^{N}\left[\frac{1}{T}\int_0^T \mu\left(r - D_{ij}\left(t\right)\right)dt\right] \tag{5-2}$$

For the discrete expression, if Δt denotes the time interval between samples, then the discrete expression of the mean CDF of the link distance becomes

$$F_D\left(r\right) = \frac{1}{N\left(N-1\right)}\sum_{i=1}^{N}\sum_{\substack{j=1 \\ j\neq i}}^{N}\left[\frac{1}{\lfloor T/\Delta t\rfloor}\sum_{k=0}^{\lfloor T/\Delta t\rfloor}\mu\left(r - D_{ij}\left(k\Delta t\right)\right)\right]. \tag{5-3}$$

Correspondingly, the discrete expression of the mean PDF of the link distance can be written as

$$f_D\left(r\right) = \frac{dF_D\left(r\right)}{dr} = \frac{1}{N\left(N-1\right)}\sum_{i=1}^{N}\sum_{\substack{j=1 \\ j\neq i}}^{N}\left[\frac{1}{\lfloor T/\Delta t\rfloor}\sum_{k=0}^{\lfloor T/\Delta t\rfloor}\delta\left(r - D_{ij}\left(k\Delta t\right)\right)\right] \tag{5-4}$$

where $\delta[\cdot]$ is an impulse function. Let Δr be the distance interval between samples for the probability mass function (PMF) of the link distance. Then the PMF of the link distance becomes

$$f_D(r_L) = P\{r_{L-1} < D \le r_L\} = F_D(L\Delta r) - F_D((L-1)\Delta r) \tag{5-5}$$
$$= \frac{1}{\lfloor T/\Delta t \rfloor} \sum_{k=0}^{\lfloor T/\Delta t \rfloor} \left[\frac{1}{N(N-1)} \sum_{i=1}^{N} \sum_{\substack{j=1 \\ j \neq i}}^{N} \left(\mu\left(r_L - D_{ij}(k\Delta t)\right) - \mu\left[r_{L-1} - D_{ij}(k\Delta t)\right] \right) \right]$$

where $r_L = L\Delta r$. Now, the asymptotic mean CDF and PDF of the link distance can be estimated from the relative frequency of the link distance obtained from the results of the simulation. The accuracy of the estimation depends on the size of samples. In the simulation, 10^7 samples have been used for the estimation of the PDF. The Gauss-Markov model is adapted for mobility, where 1000 nodes are uniformly distributed initially and the movement of a node is independent of other nodes. It is assumed that the time constant is 3 seconds and the time interval between time samples is 1 second. It is also assumed that the tuning parameter (φ) has a value of 0.7165 for the mobility model used in this simulation. Normally, the PDF can express the characteristics of the statistics in a detailed manner compared to the CDF. Therefore the PDF graph is estimated to show the characteristics of link distance. Figure 5-2 is the result of the asymptotic PDF of the link distance obtained from our simulation. The solid line indicates the result of simulation and the dotted line indicates the Beta PDF where the values of parameters *A* and *B* are respectively 2.09 and 2.61. Respectively the Beta PDF can be represented as

$$f_{Beta}(x) = \frac{\Gamma(A+B)}{\Gamma(A)\Gamma(B)} x^{A-1}(1-x)^{B-1}\Big|_{0 \le x \le 1} \tag{5-6}$$

where $0 \le x \le 1$, $\Gamma(A) = \int_0^\infty e^{-t} t^{A-1} dt$, $x = \frac{r}{2R + r_0}$, and $r_0 = 4$.

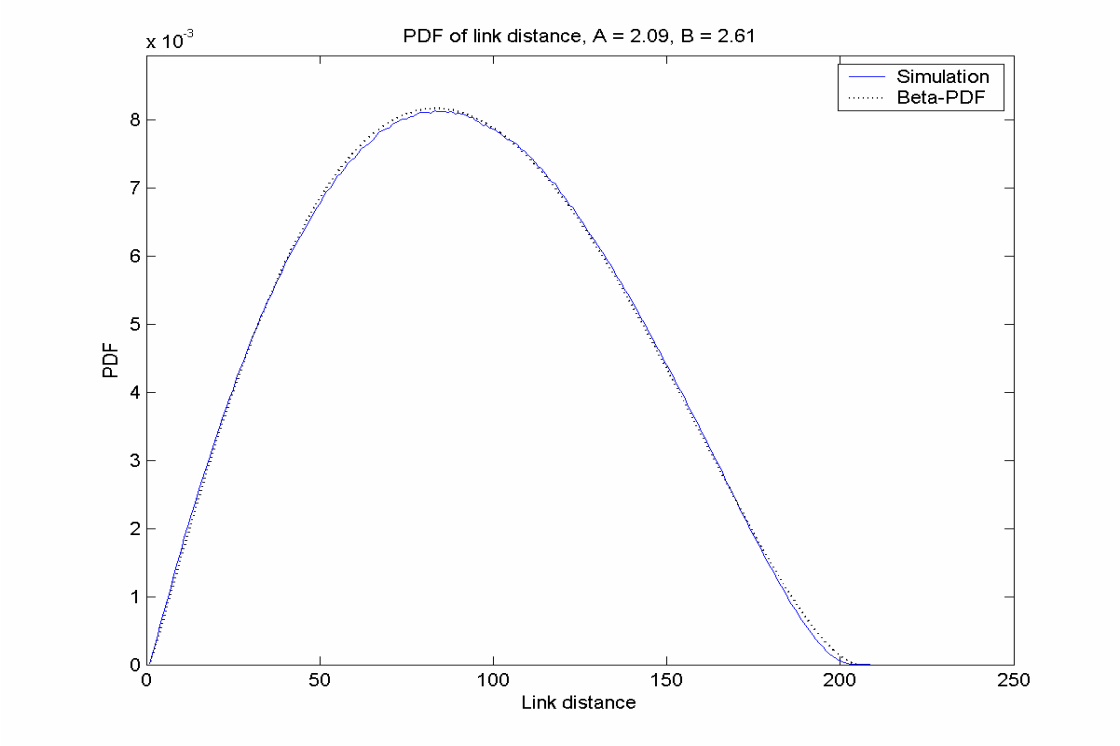

Figure 5-2: The PDF of the link distance.

The graphs in Figure 5-2 show that the PDF of the link distance adapted to the Gauss-Markov mobility model follows the Beta PDF. The value of r_0 results from the loose limitation on the network radius R. The network boundary R is not a strict limitation which means that the nodes can be located outside of the network temporarily. Therefore the maximum distance a mobile node can be located at increases with the average speed of the mobility model. The asymptotic mean CDF of the link distance ($F_D(r)$) is

$$F_D(r) \approx \frac{\Gamma(A)\Gamma(B)}{\Gamma(A+B)} \int_0^{\frac{r}{2R+r_0}} \xi^{A-1}(1-\xi)^{B-1} d\xi = F_{beta}\left(\frac{r}{2R+r_0}\right) \tag{5-7}$$

and the asymptotic mean PDF of the link distance ($f_D(r)$) becomes

$$f_D(r) \approx \frac{1}{(2R + r_0)} f_{beta}\left(\frac{r}{2R + r_0}\right) \tag{5-8}$$

where $F_{beta}(\cdot)$ is the Beta CDF and $f_{beta}(\cdot)$ is the Beta PDF.

5.3 The Distribution of the SINR

In the previous section, the asymptotic mean distribution of the link distance is calculated from a random network where N i.i.d. nodes are randomly located in a circle of radius R. The PDF of the bit error rate (BER, p) will be investigated based on the signal to interference plus noise ratio (SINR, γ). In this section the distribution of the SINR is induced from the distribution of the link distance. From (2-9) when the link distance is d, the mean SINR is

$$\gamma = E\left[X(r)\right] = \frac{\bar{P} r^{-\alpha}}{\rho N_0 W + I_0}. \tag{5-9}$$

Then the link distance expressed in terms of the SINR is

$$r = \left[\frac{\bar{P}}{\gamma(\rho N_0 W + I_0)}\right]^{\frac{1}{\alpha}}. \tag{5-10}$$

From (2-5) and (5-7) the CDF of the mean SINR becomes

$$F_{\Gamma}(\gamma) = 1 - F_{beta}\left(\frac{1}{2R + r_0}\left[\frac{\bar{P}}{(\rho N_0 W + I_0)}\right]^{\frac{1}{\alpha}}\left(\frac{1}{\gamma}\right)^{\frac{1}{\alpha}}\right). \tag{5-11}$$

The derivation of (5-11) is included in the Appendix.

Let $Z_\Gamma(\gamma) = \frac{1}{2R + r_0}\left[\frac{\overline{P}}{(\rho N_0 W + I_0)}\right]^{\frac{1}{\alpha}}\left(\frac{1}{\gamma}\right)^{\frac{1}{\alpha}}$. Then the CDF of the mean SINR is

$$F_\Gamma(\gamma) = 1 - F_{beta}(Z_\Gamma(\gamma)). \tag{5-12}$$

The PDF of the mean SINR is defined as

$$f_\Gamma(\gamma) = \frac{\partial F_\Gamma(\gamma)}{\partial \gamma}. \tag{5-13}$$

From (5-12) the PDF of the mean SINR can be obtained from

$$f_\Gamma(\gamma) = \frac{Z_\Gamma(\gamma)}{\alpha\gamma} f_{beta}(Z_\Gamma(\gamma)). \tag{5-14}$$

Table 5-1: Parameter values for estimation of the distribution of BER.

Parameters	**values**
Mean interference power (I_0)	-100 dBm
Common transmission power ($\overline{P}$)	15 dBm
Noise factor (ρ)	10
Thermal noise power (N_0)	-173.8 dBm/Hz
Bandwidth (W)	2 MHz
Path loss exponent (α)	3.5
Network radius (R)	750 m

The derivation of (5-14) is included in the Appendix. For the specific PDF of the SINR, we consider using the IEEE 802.11b preamble transmission scheme of [14], where the IEEE 802.11b preamble is transmitted using differential phase shift keying (DPSK) regardless of the modulation or rate used for the data. Table 5-1 shows the values of parameters used for the calculation of the distribution of the SINR. The mean interference power is assumed to be -100 dBm.

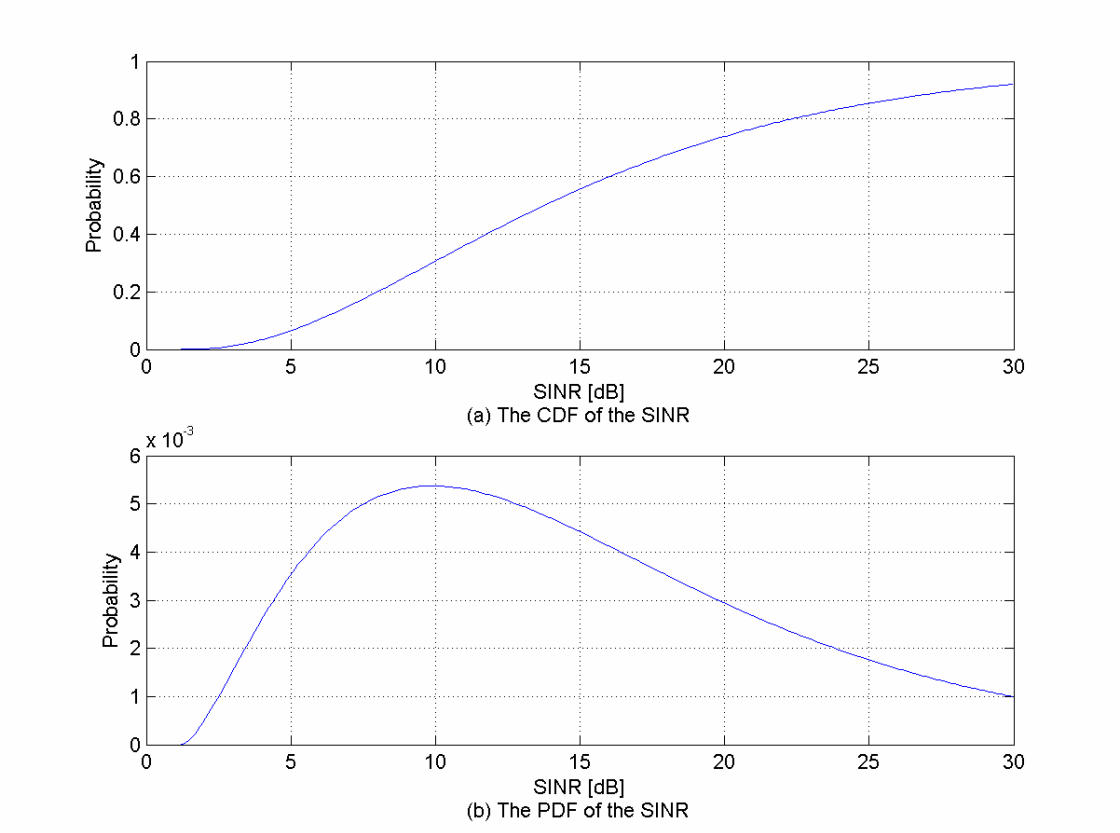

Figure 5-3: The PDF and CDF of the SINR.

Figure 5-3 has been obtained from the PDF of the link distance and the parameters in Table 5-1. The graph in Figure 4 (a) indicates the CDF of the SINR and the graph in Figure 4 (b) indicates the PDF of the SINR.

5.4 The Distribution of the BER

The calculation of the BER from the SINR for a specific wireless protocol (e.g., IEEE 802.11b) is not easy and there is no exact function to convert the SINR to BER. The complication results from the protocol multiple access scheme, synchronization algorithm, packet formant, and error control coding. Therefore, mapping functions are used to convert the SINR to BER and the approximated equations will be induced from the mapping function. Let *H* be the function that converts the SINR to the BER. Figure 5-4 is the BER chart that was obtained from the Qualnet simulator 3.7 [12].

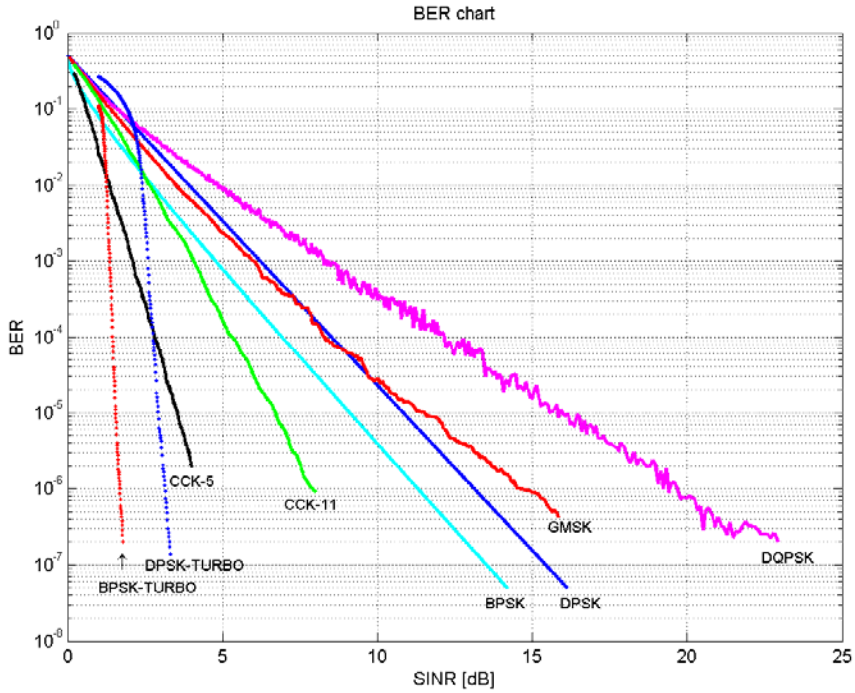

Figure 5-4: The conversion map of the SINR to BER.

The performance curves in Figure 5-4 are almost straight lines over all regions of the SINR. Therefore an approximation of *H* based on Figure 5-4 can be expressed as follows

$$p \approx a\left(E\left[X(D)\right]\right)^{b} \tag{5-15}$$

where p is the BER and $E\left[X(D)\right]$ is the mean SINR for a given link distance D. For example, the value of a for Differential Phase Shift Keying (DPSK) approximation is 0.5 and b is -4.3429. As shown in Figure 5-5, the error between the approximation equation and the mapping chart of DPSK is less than 0.001 % over all regions of the SINR.

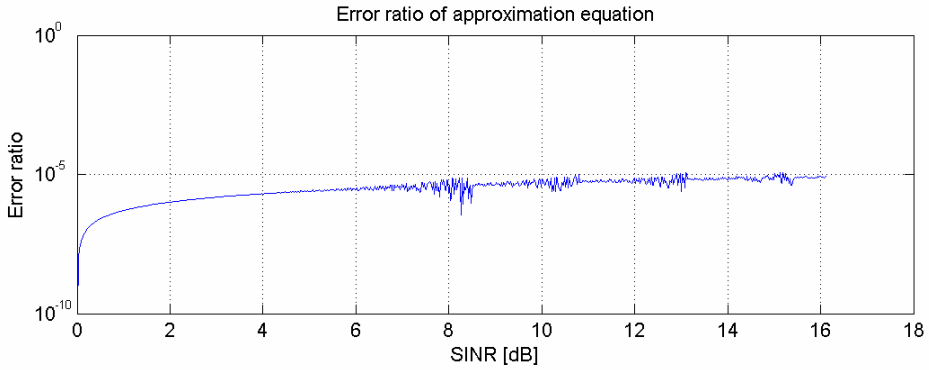

Figure 5-5: The error ratio of approximation DPSK equation based on Figure 5-4.

The approximated function (5-15) of H is an invertible function so that the distribution of mean BER can be obtained from the distribution of the mean SINR. The inverse function of H can be written as

$$H^{(-1)}(x) = \left(\frac{x}{a}\right)^{\frac{1}{b}}. \tag{5-16}$$

By combining (5-12), (5-15), and (5-16) the CDF of the mean BER can be written as

$$F_{\mathrm{B}}(p) = F_{beta}\left(\frac{1}{2R + r_0}\left[\frac{\bar{P}}{(\rho N_0 W + I_0)} \right]^{\frac{1}{\alpha}} \left(\frac{a}{p} \right)^{\frac{1}{\alpha b}} \right). \tag{5-17}$$

The derivation of (5-17) is included in the Appendix.

Let $Z_{\mathrm{B}}(p) = Z_{\Gamma}\left(H^{(-1)}(p)\right) = \frac{1}{2R + r_0}\left[\frac{\bar{P}}{(\rho N_0 W + I_0)} \right]^{\frac{1}{\alpha}} \left(\frac{a}{p} \right)^{\frac{1}{\alpha b}}$. Then the CDF of the mean BER can be written as

$$F_{\mathrm{B}}(p) = F_{beta}(Z_{\mathrm{B}}(p)). \tag{5-18}$$

The PDF of mean BER is

$$f_{\mathrm{B}}(p) = \frac{\partial F_{\mathrm{B}}(p)}{\partial p}. \tag{5-19}$$

From (5-18) and (5-19) the PDF of the mean BER becomes

$$f_{\mathrm{B}}(p) = -\frac{Z_{\mathrm{B}}(p)}{\alpha b p} f_{beta}\left(Z_{\mathrm{B}}(p)\right). \tag{5-20}$$

The derivation of (5-20) is included in the Appendix. The specific PDF of the BER is needed for the purpose of simulation. In the previous section, the 802.11b preamble transmission scheme is used for the calculation of the PDF of SINR. The IEEE 802.11b preamble is transmitted using DPSK regardless of the modulation or rate used for the data. The values of *a* and *b* in the approximation function to convert SINR to BER of DPSK are respectively 0.5 and -4.343.

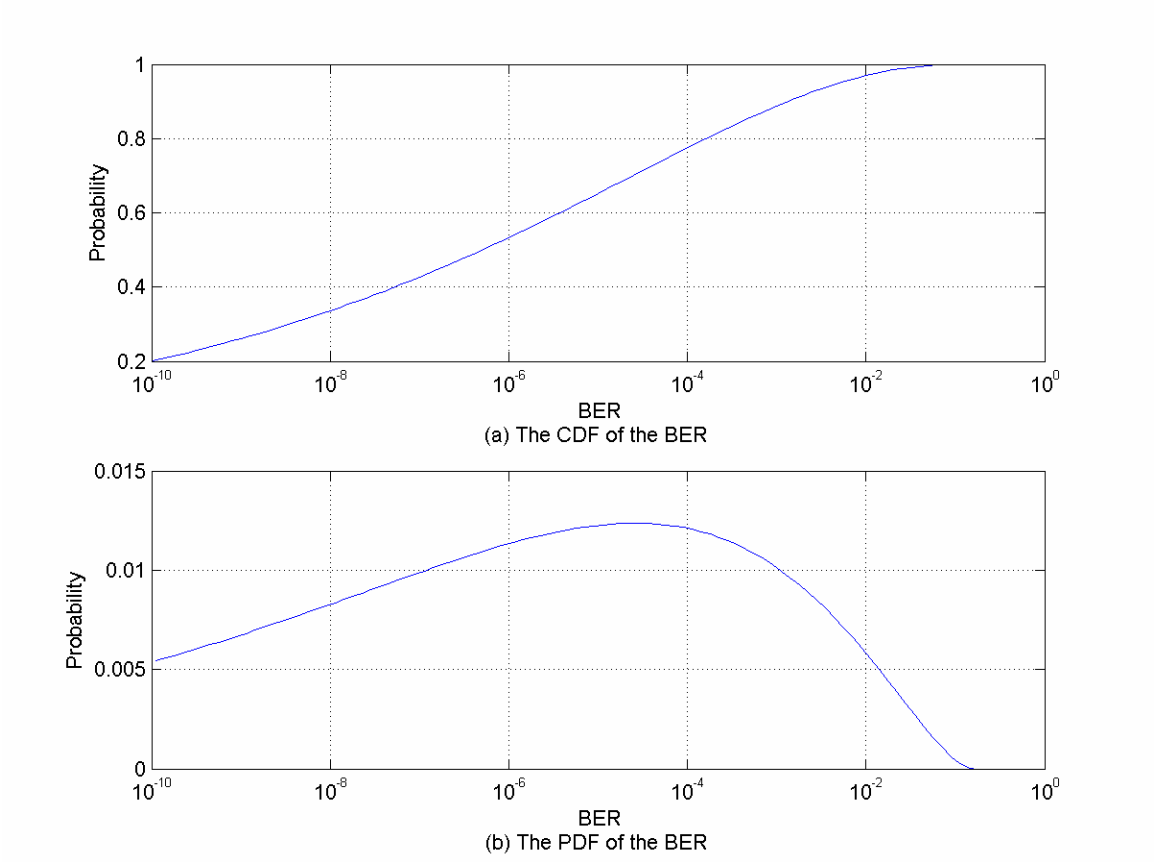

Figure 5-6: The PDF of BER.

Figure 5-6 shows the distribution of BER when the IEEE 802.11b MAC protocol is adapted. The graph in Figure 5-6 (a) indicates the CDF of the BER and the graph in Figure 5-6 (a) indicates the PDF of the BER.

Chapter 6

Derivation and Experimentation of the MANET Efficiency Applying the Mobility Model

6.1 The Optimal Packet Size

The packet size affects the performance of the wireless links due to the characteristics such as the high error rate or time varying channel condition. The optimal packet size based on the BER can be chosen by the data link protocol through the ARQ controller to maximize the communication performance (throughput). If the channel bit-error rate is known, the optimal packet size can be obtained. Throughput is defined as the amount of data (bits) transferred successfully from source to destination in a given time period. Throughput can be calculated from the data rate and packet error rate. Data is transported using packets which consist of overhead (h) and payload (k). Let P_E denote the packet error rate and p denote the BER. In this thesis, throughput is defined as the ratio of the total amount of successful payload transferred to the destination over a given time interval. Successful moving means that a received packet has no bits in error after the error control coding. The packet error rate is given in (2-14).

$$P_E = 1 - \sum_{i=0}^{c} \binom{k+h}{i} p^i (1-p)^{k+h-i} . \quad (6\text{-}1)$$

Let R_D denote the data rate. The total amount of payload received successfully is reduced by the overhead and packet errors. Considering this, the throughput can be represented as

$$\Theta = R_D \frac{k}{k+h}(1-P_E) = R_D \frac{k}{k+h} \sum_{i=0}^{c} \binom{k+h}{i} p^i (1-p)^{k+h-i} . \quad (6\text{-}2)$$

In this optimization problem the objective function is to maximize the throughput, the control variable is the packet size (k) and h is constant. If (6-2) is differentiable, then the optimal packet size to maximize the throughput can be obtained by taking the partial derivation of (6-2) ($\frac{\partial \Theta}{\partial k} = 0$). It is not easy to solve the equation $\frac{\partial \Theta}{\partial k} = 0$ as a closed form solution may not exist. The optimal packet size for a given p can be obtained by using a numeric search algorithm which finds the packet size to maximize the throughput for a given p. Figure 6-1 (a) shows the throughput using the packet size k for a given p, where the overhead size is 272 bits (34 bytes) and the value of correctable bits (c) is 5 bits. The asterisk markers in Figure 6-1 (a) represent the packet size that maximizes the throughput for a given p. By searching the asterisk markers it is possible to obtain the optimal packet size for a given p. For example, k_{opt} is 204 bits when p is 10^{-2}, and k_{opt} is 14560 bits when p is 10^{-4}. Figure 6-1 (b) shows the optimal packet size based on the BER. The optimal packet size can not be perfectly obtained because the channel bit error rate cannot be known in advance. Therefore, estimations are used or a predictive algorithm can be applied.

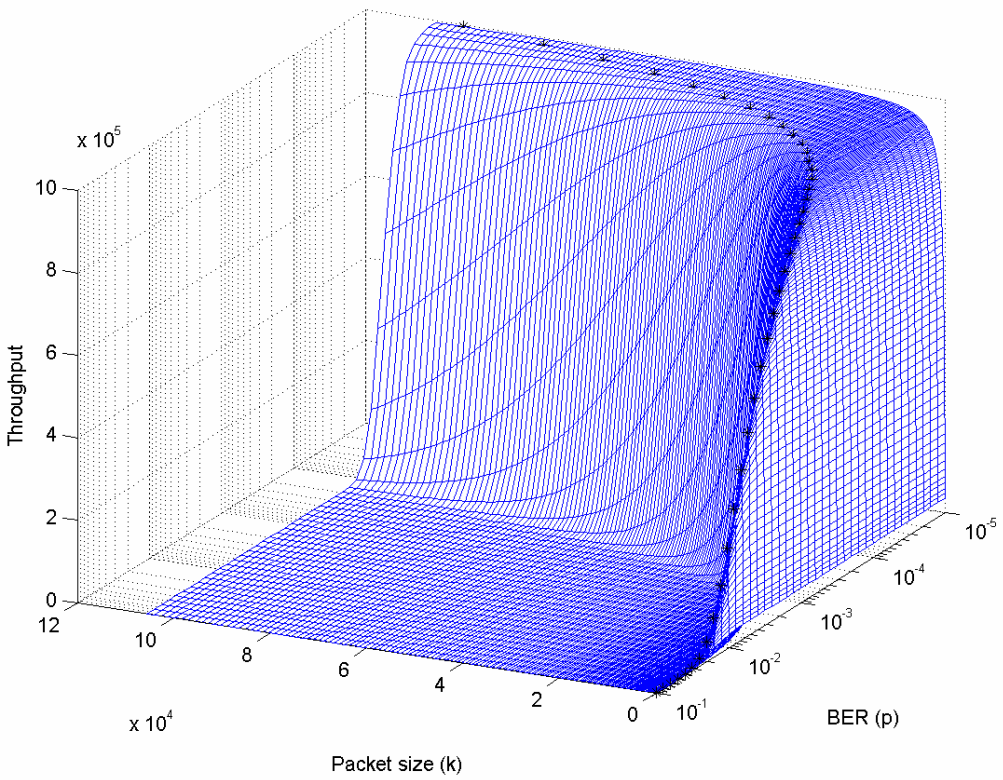

(a) Throughput for a given *p*.

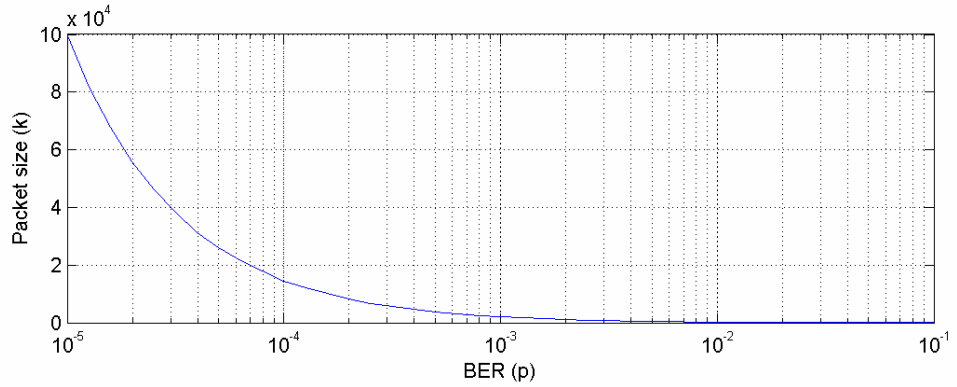

(b) The optimal packet size for a given *p*.

Figure 6-1: The throughput and optimal packet size for a given *p*.

This is commonly the case for wireless channels where the channel condition is time varying and unpredictable. In [6] an algorithm which optimizes the size of the packets to increase the performance has been developed, where the channel condition can not be known in advance. The channel condition is estimated from the number of packets that required retransmission, which will be then used to obtain to the maximize performance. In [6], the channel condition is estimated based on an assumption of the uniform distribution of the BER. In Chapter 3 the distribution of the BER from the Gauss-Markov mobility model is obtained. In this chapter, the distribution of the BER obtained in Chapters 3 and 5 is used for the extension of the algorithm of [6] to consider the effect of mobility. By adapting the distribution of the BER from mobility, it is possible to increase the performance of the wireless link which is erroneous.

6.2 Analysis of the Protocol Efficiency

The optimal packet size can be chosen based on the estimated channel condition to maximize the performance of a protocol. An implementation of an optimal ARQ protocol where only packets containing errors are retransmitted is assumed [6]. Let ε denote the efficiency of a protocol, which is the ratio of achievable throughput to the data rate, as a metric of protocol performance.

$$\varepsilon(k) = \frac{\Theta}{R_D} = \frac{k}{(h+k)} \sum_{i=0}^{c} \binom{k+h}{i} p^i (1-p)^{k+h-i} \qquad (6\text{-}4)$$

The BER (p) value can not be obtained in advance. So it will be estimated from the number of retransmission requests (Q) and the number of packet transmissions (M). If the BER (p) is estimated from Q and M, the conditional efficiency can be expressed by taking an average over all possible values of the BER for a given Q. It is assumed that p is constant over the period of interest. Then the efficiency of the protocol with Q retransmissions can be written

$$\varepsilon_Q(k) = \int_{-\infty}^{\infty} \varepsilon(k) P\left[p|Q\right] dp = \int_0^1 \left(\sum_{i=0}^{c} \frac{k}{k+h} \binom{k+h}{i} p^i (1-p)^{k+h-i} \right) P\left[p|Q\right] dp . \quad (6\text{-}5)$$

From Bayes' theorem, the conditional probability of p given Q, $P[p|Q]$, becomes

$$P\left[p|Q\right] = \frac{P\left[Q|p\right] f_{\mathrm{B}}(p)}{P[Q]} \quad (6\text{-}6a)$$

and $P[Q]$ can be written as

$$P[Q] = \int_0^1 P\left[Q|p\right] f_{\mathrm{B}}(p)\, dp . \quad (6\text{-}6b)$$

In this chapter, it is assumed that each bit error occurs independently. Let $\hat{k}$ be the packet size used in the previous M transmissions. Then the packet error rate in reference to the previous packet size (k_{pre}) is

$$\hat{P}_E = 1 - \sum_{i=0}^{c} \binom{k_{pre}+h}{i} p^i (1-p)^{k_{pre}+h-i} . \quad (6\text{-}7)$$

The conditional probability $P[Q|p]$ is the probability that exactly Q retransmissions occur among M transmissions for a given p .

The conditional probability ($P[Q|p]$) can be calculated from Bernoulli trials, as

$$P[Q|p] = \binom{M}{Q} \left(\hat{P}_E\right)^Q \left(1-\hat{P}_E\right)^{M-Q}. \tag{6-8}$$

The expected efficiency of the protocol for a given value of Q can be calculated from (6-4) ~ (6-8). When Q and M are known from the previous history, the efficiency of the algorithm using the current packet size of k is

$$\varepsilon_Q(k) = \frac{k}{(k+h)} \int_0^1 \frac{(1-P_E)}{P[Q]} \binom{M}{Q} \left(\hat{P}_E\right)^Q \left(1-\hat{P}_E\right)^{M-Q} f_{\mathrm{B}}(p)\, dp \tag{6-9}$$

where $\hat{P}_E = 1 - \sum_{i=0}^{c} \binom{k_{pre}+h}{i} p^i (1-p)^{k_{pre}+h-i}$, k_{pre} is the packet size used in the previous history, $P_E = 1 - \sum_{i=0}^{c} \binom{k+h}{i} p^i (1-p)^{k+h-i}$, and k is the current packet size. The variable Q, M, and k_{pre} are used for the estimation of the channel condition, ($P[p|Q]$), based on which the protocol will decide the packet size for the next transmission.

If the BER is known, the performance of a single iteration can be easily evaluated by (6-4). The optimal packet size can be directly calculated from (6-3) for a given p which can then be used to evaluate the optimal efficiency. Let k_{opt} be the optimal packet size for a given BER. Then the efficiency using k_{opt} for a given p is

$$\varepsilon_{opt}(p) = \left(\frac{k_{opt}}{k_{opt}+h}\right)\sum_{i=0}^{c}\binom{k_{opt}+h}{i}p^{i}(1-p)^{k_{opt}+h-i} \tag{6-10}$$

The optimum efficiency can be obtained by taking expectation of $\varepsilon_{opt}(p)$ over the distribution of BER. Then the optimum efficiency can be written as

$$\varepsilon_{opt} = \int_{0}^{1} \varepsilon_{opt}(p) f_{\mathrm{B}}(p) dp \,. \tag{6-11}$$

This is the case where the BER is unknown, but Q, M, and k_{pre} are known from previous history. So the optimal packet size can be decided by the protocol based on these values. Let $k_{pro}(Q)$ be the packet size to maximize equation (6-9) for a given value of Q that is equal to the number of retransmission requests that occurred during the previous M transmissions. So the packet size chosen by the protocol becomes

$$k_{pro}(Q) = \varepsilon_{Q}^{(-1)}\left[\max\left(\varepsilon_{Q}(k)\right)\right] \tag{6-11}$$

where $\varepsilon_{Q}^{(-1)}(\cdot)$ is the inverse function of $\varepsilon_{Q}(\cdot)$. A general solution to maximize equation (6-9) is difficult to derive. However, for specific values of Q, M, and k, equation (6-9) can be solved numerically. $k_{pro}(Q)$ can be found using a numerical search algorithm. Figure 6-2 shows the efficiency ($\varepsilon_{Q}(k)$) using the packet size k when the number of retransmission requests is Q. In the previous history, the packet size (k_{pre}) is 544 bytes, the number of transmissions (M) is 50, the value of correctable bits (c) is 0 bits. The asterisk markers represent the packet size needed to maximize the efficiency of the

protocol for a given Q, which was chosen by a numerical search algorithm. For example, $k_{pro}(Q)$ is 7410 bits when Q is 1, $k_{pro}(Q)$ is 1440 bits when Q is 20.

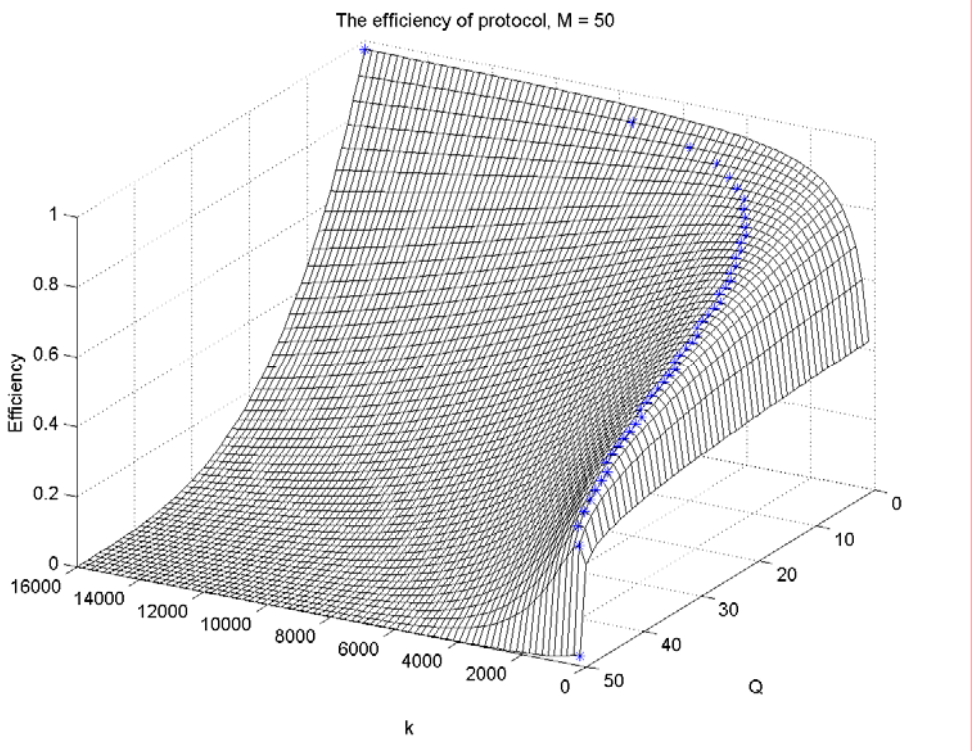

Figure 6-2: The efficiency for a given Q.

The efficiency of the algorithm that chooses the packet size to maximize the efficiency for a given Q can be calculated by taking the expectation of $\varepsilon_Q(k_{pro}(Q))$ over the distribution of Q, where $k_{pro}(Q)$ is the optimal value of k chosen by the algorithm for a given value of Q. The efficiency of the algorithm choosing $k_{pro}(Q)$ is

$$\varepsilon_{pro} = \sum_{Q=0}^{M} \varepsilon_Q\left(k_{pro}(Q)\right) P[Q] \tag{6-12}$$

where $P[Q] = \int_0^1 \binom{M}{Q} \left(\hat{P}_E\right)^Q \left(1-\hat{P}_E\right)^{M-Q} f_{\mathrm{B}}(p)\, dp$.

A specific protocol is needed for the analysis of the algorithm proposed in this thesis. For this reason, the IEEE 802.11 MAC protocol [14] is used for the analysis in this thesis and the parameter values were set to follow the default values of the Qualnet simulator [12]. Table 6-1 shows the default parameter values of the Qualnet simulator.

Table 6-1: Default parameter values of the Qualnet simulator.

Parameter	**Values**
Network size	1500m×1500m
Packet size (application)	512 bytes
Data rate (R_D)	1 Mbps
Bandwidth (W)	2 MHz
Transmission power ($\overline{P}$)	15 dBm
Receive sensitivity (P_{sen})	-89 dBm
Noise factor (ρ)	10.0
Temperature	290.0 K°

For the various environments, the path loss exponent varies from 2 to 6, the path loss exponent is set to 2 for air-to-air free space and 4 for ground-to-ground free space communication. From (2-11), the average interference must be less than the receive sensitivity to satisfy the condition that the carrier sensing range is finite. Also (2-11) shows that the interference power can exceed the receive sensitivity temporally but the average interference can not exceed the receive sensitivity. In the Qualnet simulator, the propagation limit is set to -111 dBm for channel 0, which means that the Qualnet simulator ignores the power that is less than -111 dBm. Therefore, the average

interference is set from -110 dBm to -90 dBm to generate various noisy channels. To examine various situations using different packet sizes, three types of packet sizes for the previous history are considered in the simulation: the minimum payload size, the default value, and the maximum payload size.

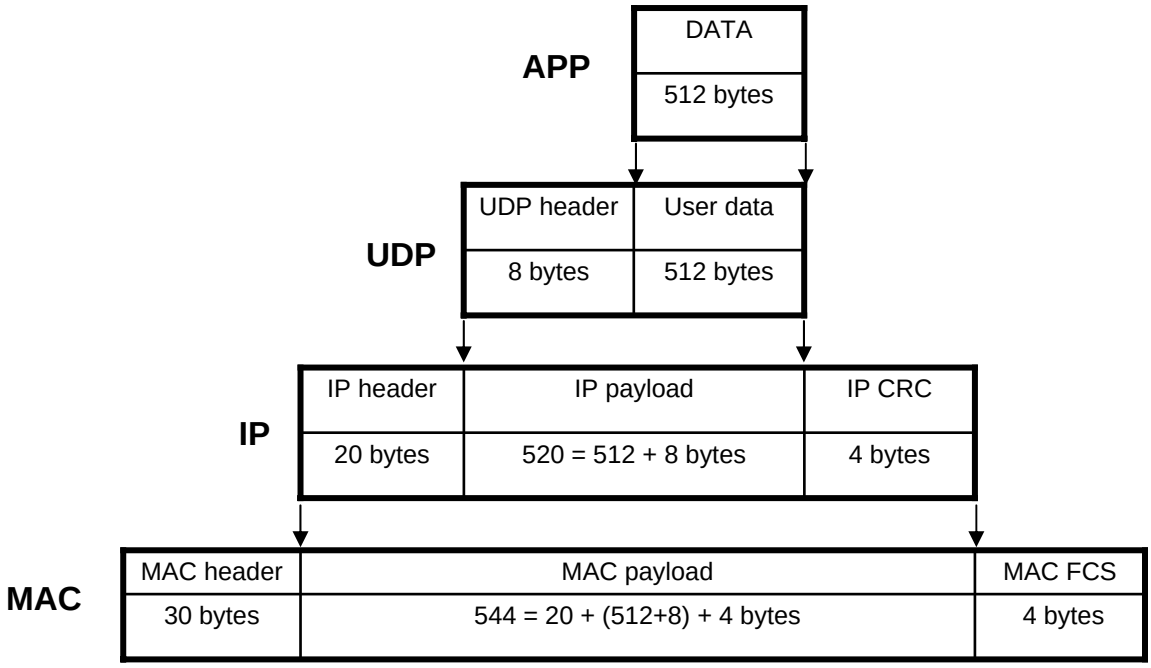

Figure 6-3: Packet format of sublayers.

Figure 6-3 shows the encapsulation schemes of an application packet over the IEEE 802.11 MAC protocol, User Datagram Protocol (UDP), and Internet protocol (IP). If the packet size of an application layer data is 512 bytes, which is the default value in the Qualnet simulator, the packet size of the MAC layer becomes 578 bytes, where the MAC payload size (k) is 544 bytes and the MAC overhead (h) size is 34 bytes. The minimum MAC payload size is 32 bytes when the size of the application layer data is 0 bytes and the maximum size of the MAC payload is 2312 bytes, as defined in [14].

Table 6-2: Parameter values for the simulation.

Parameters	**values**
Mean interference power (I_0)	-110 ~ -90 dBm
Common transmission power ($\overline{P}$)	15 dBm
Noise factor (ρ)	10
Thermal noise power (N_0)	-173.8 dBm/Hz
Bandwidth (W)	2 MHz
Path loss exponent (α)	2, 3, 4, 5
Network radius (R)	750 m
Number of history packets (M)	50 packets
Previous packet size (k_{pre})	32, 544, 2312 bytes
Packet overhead size (h)	34 byte
Correctable error bits (c)	16 bits
Packet size (k)	10 ~ 28600 bits
BER (p)	10^{-10} ~ 1

Table 6-2 shows the parameter values used in the simulation. Thermal noise is calculated for a temperature value of 290 K° and a bandwidth of 2 MHz. In the simulation, the network is circular in shape and the radius is 750 m. The range of packet size is from 10 to 28600 bits and the BER is considered from 10^{-10} to 1. The maximum correctable error bits is assumed to be 16 (i.e., 2 bytes), where the MAC frame check sequence (FCS) is 4 bytes based on the Reed-Solomon (RS) code which has the ability to correct symbol errors up to half the number of parity bytes [19].

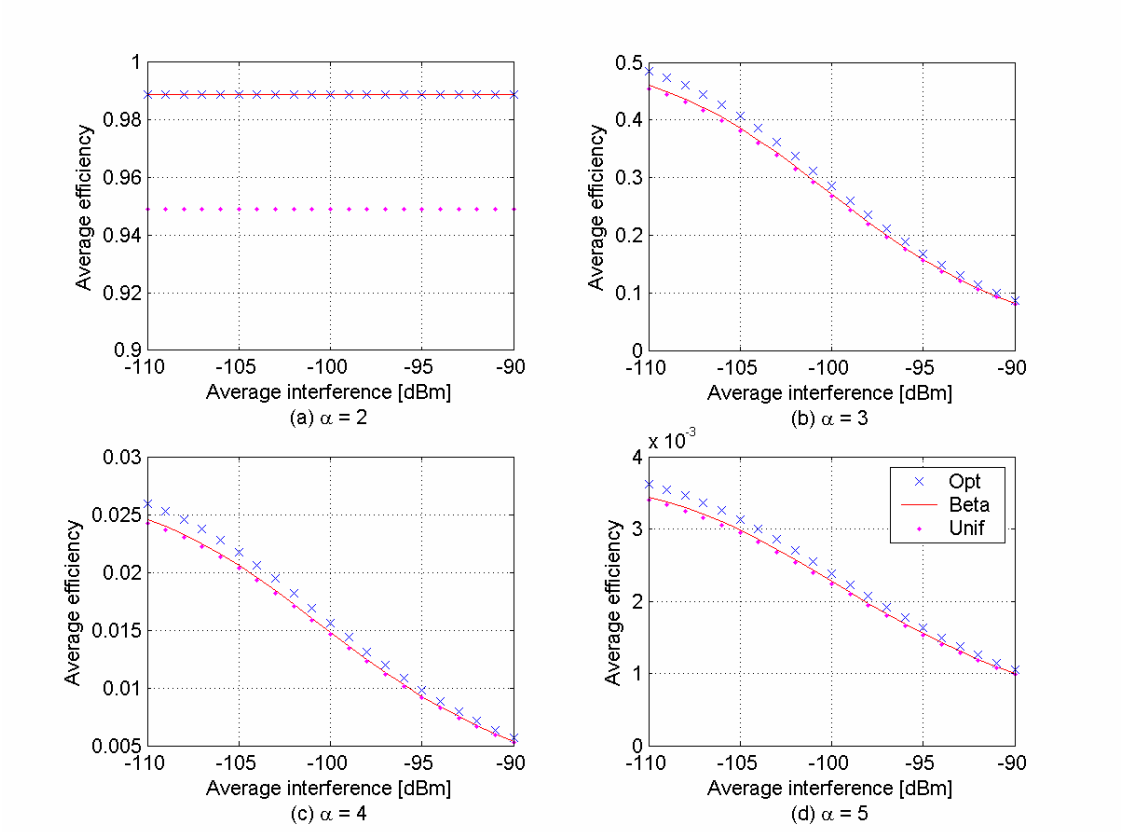

Figure 6-4: The average efficiency (k_{pre} = 544 bytes).

Figure 6-4 shows the average efficiencies of various environments using the previous packet size of 578 bytes (payload size is 544 bytes). The performance curve indicated by cross marks in Figure 6-4 represents the optimal average efficiency, which is the theoretical upper bound. The performance curve drawn as a solid line represents the average efficiency of the proposed algorithm in this thesis, which uses the information of the Beta distribution of the BER, and the performance curve indicated by dot marks represent the average efficiency of the algorithm in [6] which uses an uniform PDF of BER. Figure 6-4 (a) shows the performance curve of free space, where a path loss exponent of 2 is assumed. Figure 6-4 (b) shows the performance curve of an urban area, where a path loss exponent of 3 is assumed, Figure 6-4 (c) shows the performance curve

of a shadowed urban area, where a path loss exponent of 4 is assumed, and Figure 6-4 (d) shows the performance curve in a building, where a path loss exponent of 5 is assumed. We can observe that the algorithm proposed in this thesis is more efficient than the algorithm in [6] over various environments.

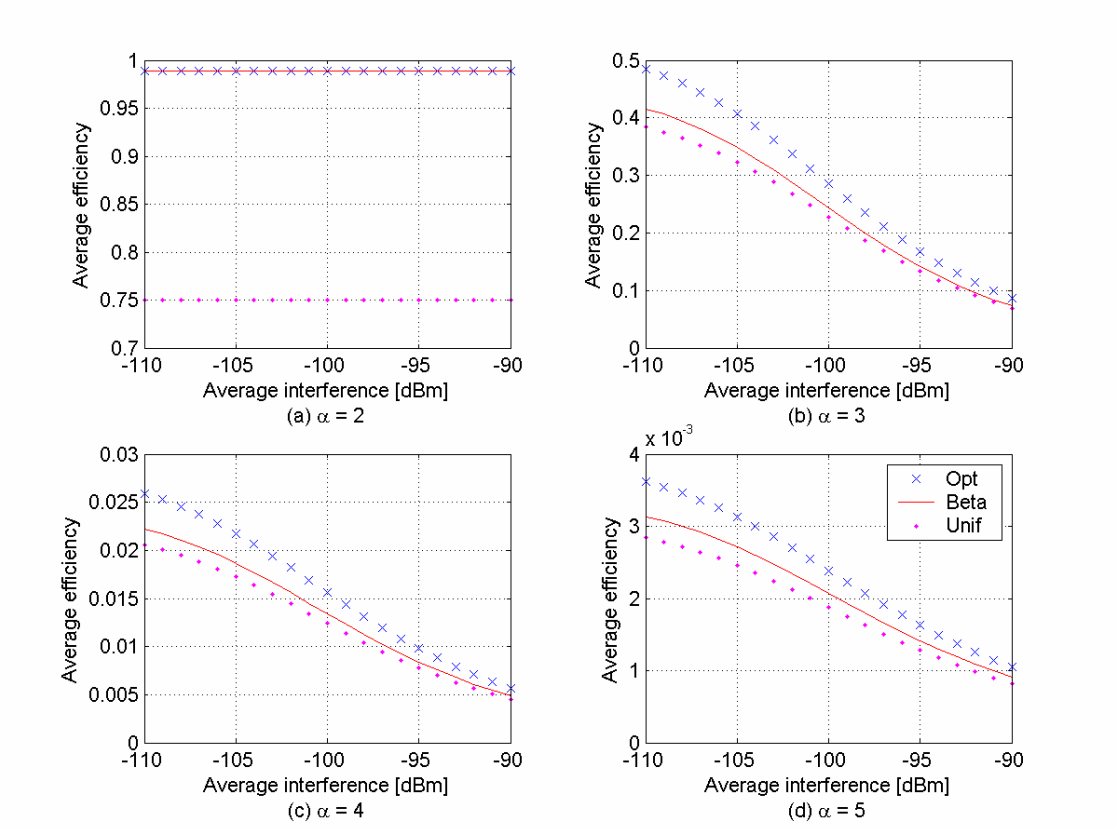

Figure 6-5: The average efficiency (k_{pre} = 32 bytes).

Figure 6-5 shows the average efficiencies of various environments using the previous packet size of 66 bytes (payload size is 32 bytes). When k_{pre} equals 32 bytes, the proposed algorithm gives a larger improvement than the case of k_{pre} = 544 bytes. This is because, if k_{pre} is 32 bytes, the total number of history bits reduced by about nine times compared to the case of k_{pre} = 544 bytes. The small number of history bits produces a

poor channel estimation in the algorithm of [6]. Therefore the performance of the algorithm in [6] of Figure 6-5 is much lower than the performance of the algorithm in [6] of Figure 6-4. The performance of the algorithm in this thesis in Figure 6-5 shows the degraded performance under short history bits but it is higher than the performance of the algorithm in [6] regardless of history sizes.

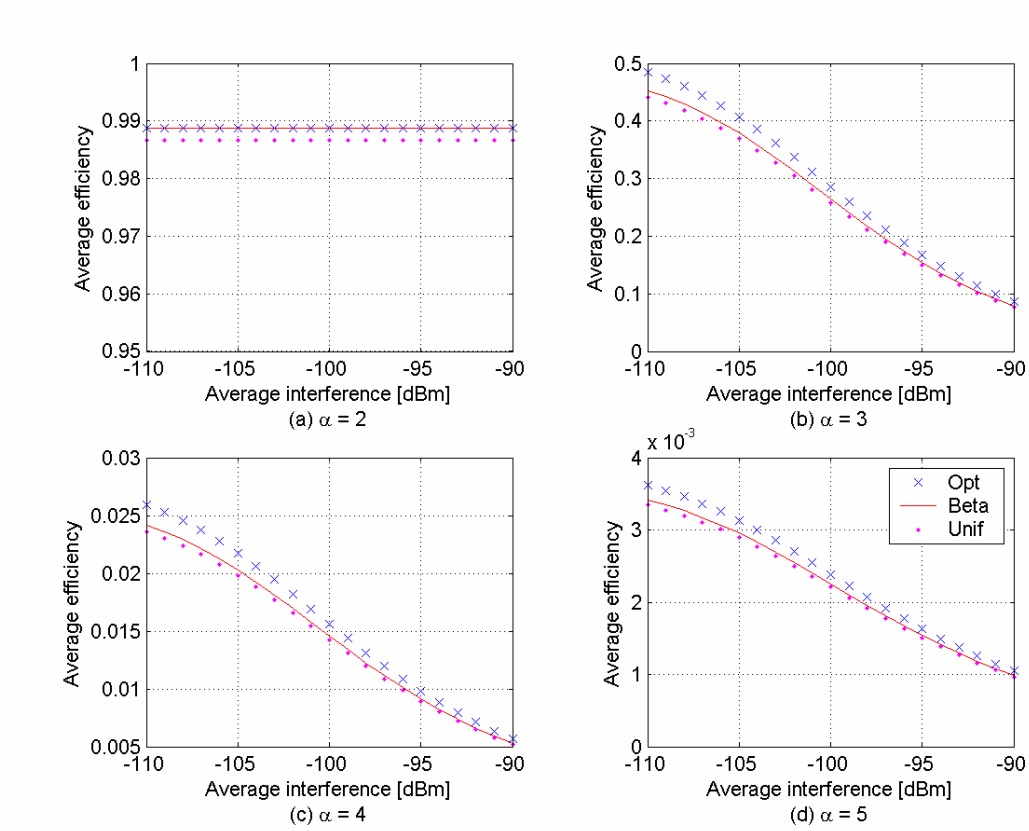

Figure 6-6: The average efficiency (k_{pre} = 2312 bytes).

Figure 6-6 shows the average efficiency based on various environments using the previous packet size of 2346 bytes (payload size is 2312 bytes), where the number of history bits is about four times larger than the case of k_{pre} = 544 bytes. Both the algorithms give an almost optimal performance based on a long history, but still the performance of the algorithm proposed in this thesis is higher than the performance of the

algorithm in [6]. From the above observations, it is found that when the average interference increases, the average efficiency decreases, and also when the path loss exponent increases, the efficiency decreases. Let the efficiency ratio (ε_{ratio}) be the ratio of the average efficiency of an algorithm to the optimal average efficiency. Then the efficiency ratio can be written as

$$\varepsilon_{ratio} = \frac{\varepsilon_{pro}}{\varepsilon_{opt}} \times 100 . \tag{6-13}$$

The optimal efficiency is the upper bound of the available efficiency. Then the efficiency ratio represents how close the performance is to the upper bound of the efficiency.

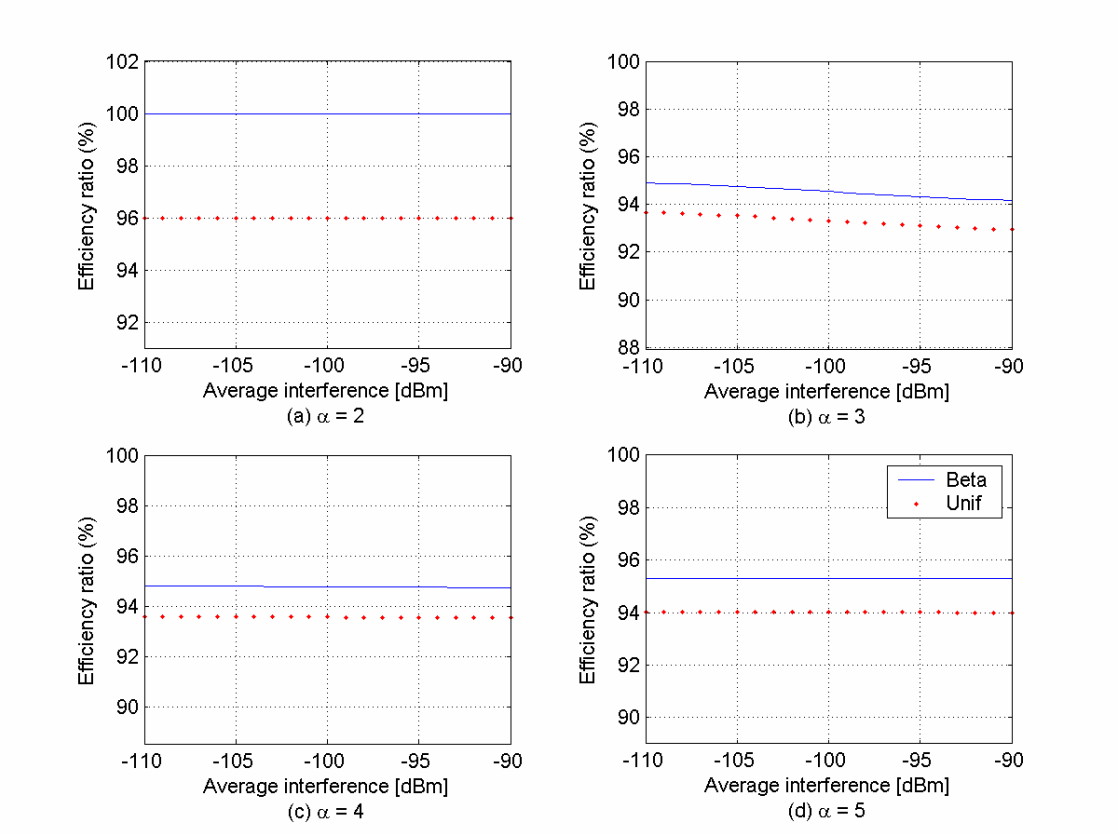

Figure 6-7: The efficiency ratio (k_{pre} = 544 bytes).

Figure 6-7 shows the efficiency ratio for a previous payload size of 544 bytes. The solid line in Figure 6-7 represents the performance of the algorithm proposed in this thesis, which uses the Beta PDF of the BER. The dot marker in Figure 6-7 represents the performance of the algorithm in [6], which uses the uniform PDF of the BER. From Figure 6-7, it is shown that when α =2, the efficiency ratio of the algorithm developed in this thesis results in an approximate 4 % higher performance compare to applying the algorithm in [6], and when α >2, the efficiency ratio of the algorithm in this thesis is about 1.5 % higher than the performance of the algorithm in [6].

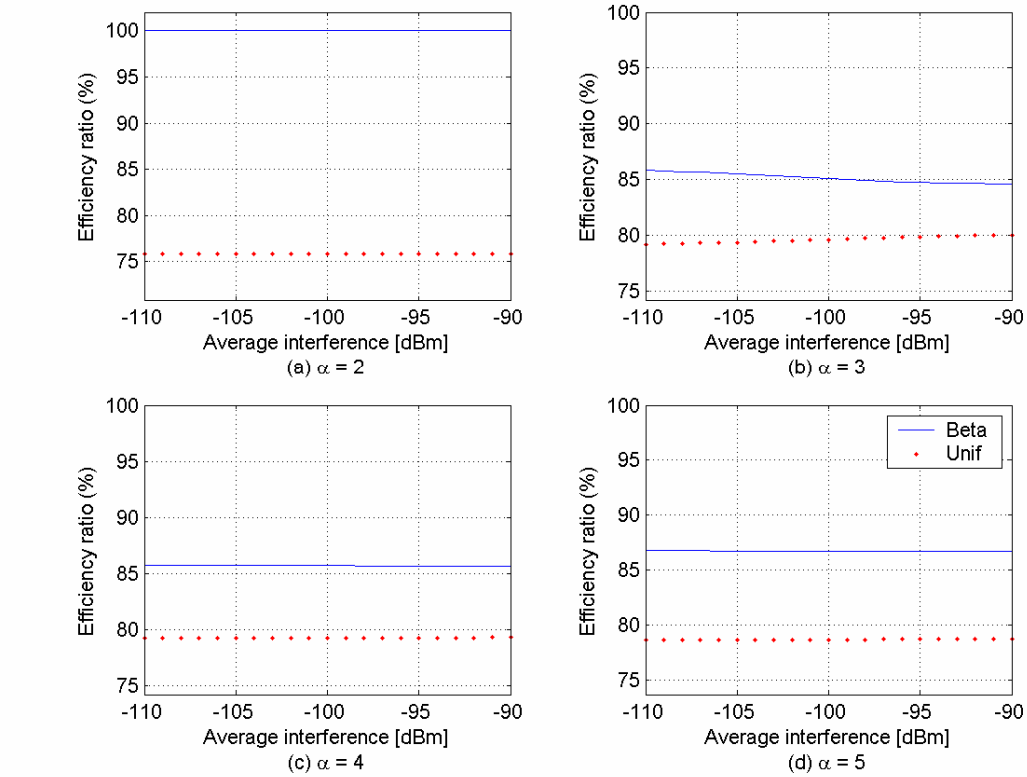

Figure 6-8: The efficiency ratio (k_{pre} = 32 bytes).

Figure 6-8 represents the efficiency ratio when the minimum MAC payload (k_{pre} = 32 bytes) is used as the previous payload size, which means the use of relatively short

history bits. Figure 6-8 shows that when α =2, the efficiency ratio of the algorithm in this thesis is about 24 % higher than the performance of the algorithm in [6], and when α >2, the efficiency ratio of the algorithm in this thesis is about 7 % higher than the performance of the algorithm in [6]. When the previous payload size is the minimum MAC payload size, the performances of the two algorithms are degraded compared to the use of 544 bytes as the previous payload size, and the efficiency ratio of the algorithm developed in this thesis is much higher than the efficiency ratio of the algorithm in [6].

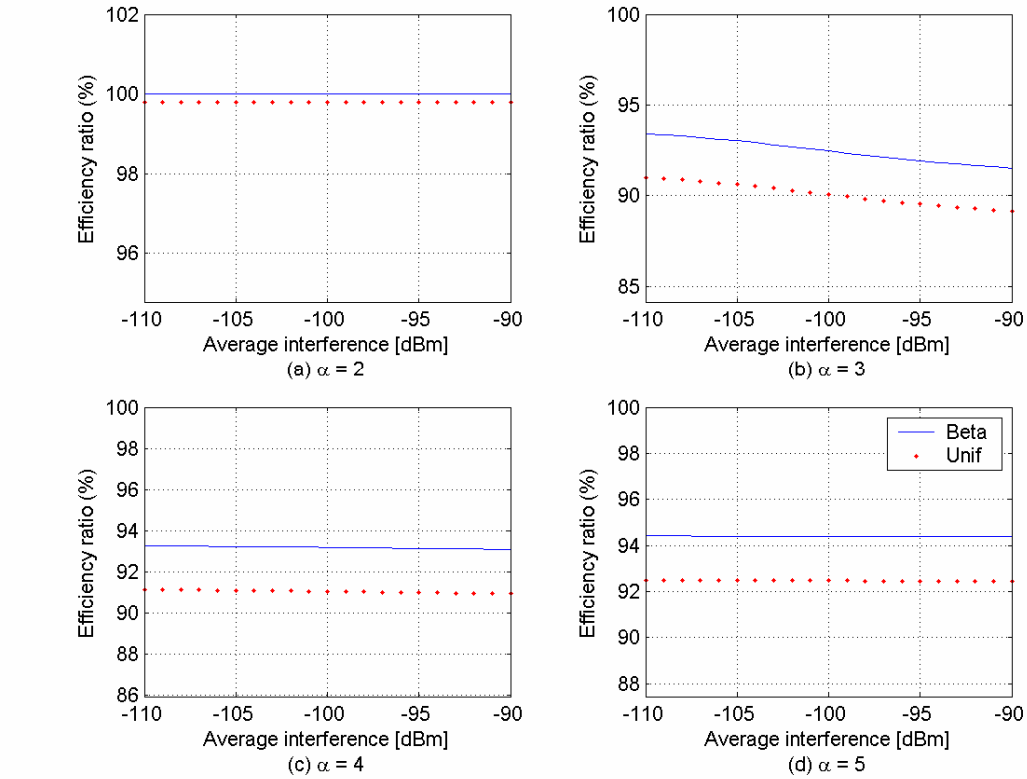

Figure 6-9: The efficiency ratio (k_{pre} = 2312 bytes).

Figure 6-9 represents the efficiency ratio when the maximum MAC payload (k_{pre} = 2312 bytes) is used as the previous payload size which means the use of relatively long history

bits. Figure 6-8 shows that when α =2, the efficiency ratio of the two algorithms are almost optimal, and when α >2, the efficiency ratio of the algorithm in this thesis is about 2 % higher than the performance of the algorithm in [6]. From Figure 6-7 to Figure 6-9, it is found that when the size of the history bits increases, the efficiency ratio increases, and when the path loss exponent increases, the efficiency ratio decreases. When the size of history bits decrease, the difference between the efficiency ratio of the two algorithms increase. The difference is almost the same over all average interference regions.

Let $E[\varepsilon_{ratio}]$ be the average efficiency ratio over the entire interference region. Then the average efficiency ratio can be written as

$$E[\varepsilon_{ratio}] = \frac{1}{N}\sum_{i=1}^{N}\varepsilon_{ratio}(i) \tag{6-14}$$

where $\varepsilon_{ratio}(i)$ represents the efficiency ratio of the i^{th} average interference in the Figures and N is 21. For example, $\varepsilon_{ratio}(1)$ represents the efficiency ratio of an average interference of -110 dBm. Figure 6-10 shows the average efficiency ratio of the two algorithms. The solid line with markers represents the average efficiency of the algorithm proposed in this thesis, and the dotted line with markers represents the average efficiency of the algorithm in [6]. The graph with dot markers represents the performance for the case of k_{pre} = 32 bytes, the graph with cross markers represents the performance for the case of k_{pre} = 544 bytes, and the graph with triangle markers represents the performance for the case of k_{pre} = 2312 bytes.

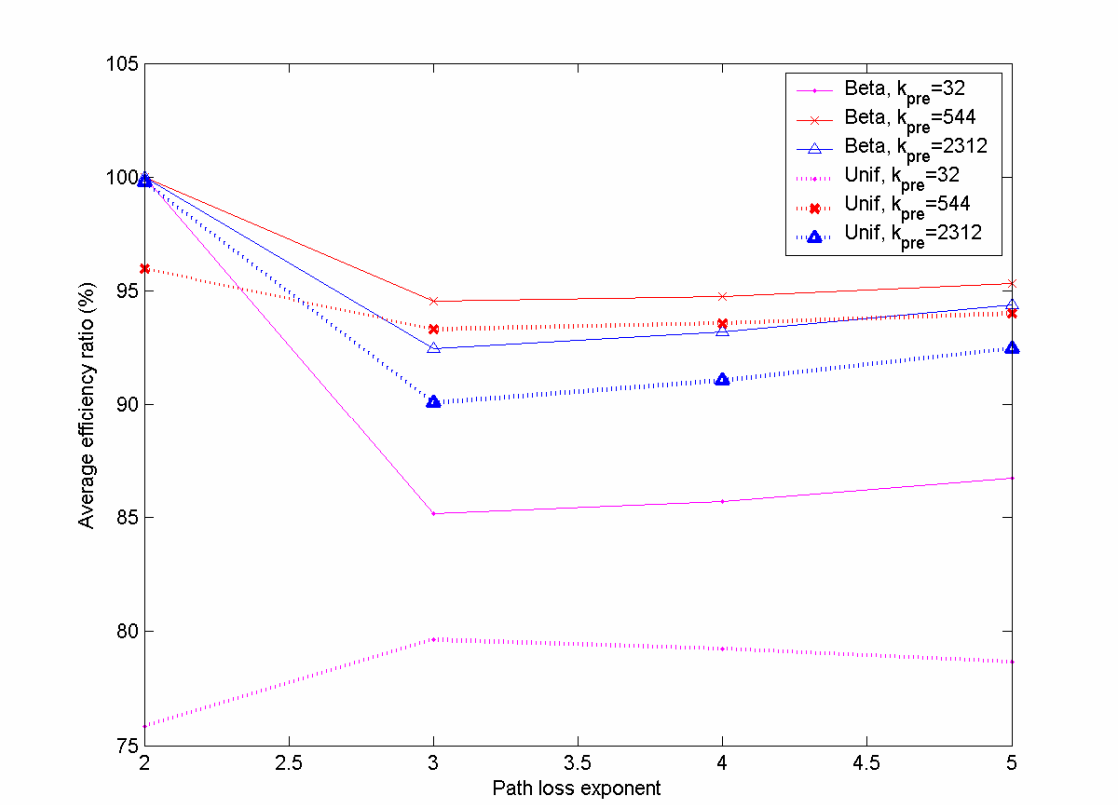

Figure 6-10: The average efficiency ratio.

In a free space environment (α =2), the performance of the algorithm proposed in this thesis is almost optimal regardless of the history size, but the performance of the algorithm in [6] is close to optimal when the size of history is large. The performance of the algorithm in [6] with k_{pre} = 32 bytes is significantly degraded compare to the use of other previous payload sizes. Figure 6-10 reveals that the average efficiency ratio of the algorithm in this thesis is always higher than the average efficiency ratio of the algorithm in [6], regardless of environments and history sizes. Table 6-3 shows the improvement which is the surplus average efficiency ratio of the average efficiency ratio of the algorithm in this thesis over the average efficiency ratio of the algorithm in [6].

Table 6-3: The performance gain obtainable from the algorithm proposed in this thesis.

The previous payload size	**Path loss exponent**			
	α =2	α =3	α =4	α =5
k_{pre} = 32 bytes	24.15 %	5.53 %	6.45 %	8.06 %
k_{pre} = 544 bytes	4.03 %	1.23 %	1.20 %	1.29 %
k_{pre} = 2312 bytes	0.21 %	2.40 %	2.14 %	1.92 %

When k_{pre} = 32 bytes and α =2 the improvement is extremely high. In the case of free space and short history, the algorithm proposed in this thesis shows a much better performance than the algorithm in [6]. In the case of long history and non-free space, the algorithm proposed in this thesis still shows better performance than the algorithm in [6]. The observation of the simulation results of various environments show that by applying the distribution of the BER, which has been done in this thesis, it is possible to improve the throughput performance in MANETs beyond the performance obtained when applying an uniform distribution.

Chapter 7

Conclusion

In this thesis the algorithm of [6] is extended by applying the non-uniform distribution of the BER derived from the mobility model and the channel error rate model. In the developed algorithm, the packet size is adapted to maximize the communication performance through the selective-reject ARQ protocol. The optimal packet size is selected based on an algorithm utilizing the estimation of the channel from the number of retransmission requests and the link statistics obtained from the mobility pattern. By adapting the non-uniform distribution of the BER obtained from mobility pattern, it is possible to estimate more accurate channels conditions from the number of retransmission requests and to improve the throughput and utilization performance of MANET communication systems.

In this thesis, it is found that the distribution of the link distance well fits the Beta distribution function for wireless circular area networks, and the distribution of the BER is obtained from a mathematical derivation based on the distribution of the link distance. Also it is shown that the performance improvement of the algorithm proposed in this

thesis exceeds the throughput and utilization performance compared to when using the uniform BER distribution model of [6].

The results of this thesis show that the results of [6] are not sufficient in estimating or controlling wireless MANET operations, and through the derivation and experimentation of the MANET mobility model a performance model significantly closer to the theoretical bound can be obtained for MANET communication systems.

In future research of MANET communication systems, the unpredictable topology change caused by the node mobility was shown to significantly affect the performance in multihop wireless MANET communications. Our study will be extended to include the link change probability and link life time for a performance improvement in MANETs. The future research will also utilize the derived distribution of link distance obtained in this thesis.

References

[1] H. Xiao, K.C. Chua and K. G. W. Seah, "A Flexible Quality of Service Model for Mobile Ad Hoc Networks," *The handbook of ad hoc wireless networks.* CRC Press, 2003.

[2] S. Lee and A. T. Campbell, "INSIGNIA: In-band signaling support for QoS in mobile ad hoc networks," in *Proc. of the 5 th International Workshop on Mobile Multimedia Communications*, 1998.

[3] R. Sivakumar, O. Sinha and V. Bharghavan, " CEDAR: a Core-Extraction Distributed Ad Hoc Routing Algorithm," *IEEE Journal on Selected Areas in Communications, Special Issue on Ad Hoc Networks*, vol. 17, no. 8, 1999.

[4] Q. Xue and A. Ganz, "Ad hoc QoS on-demand routing (AQOR) in mobile ad hoc networks," *Journal of Parallel and Distributed Computing*, vol. 63, no.2, p.154-165, Feb. 2003.

[5] S. Kuppa and R. Prakash, " IEEE 802.11 DCF scheme with knowledge-based backoff," in *Proc. IEEE Wireless Communications and Networking Conference*, New Orleans, Louisiana, USA, Mar. 13-17, 2005.

[6] E. Modiano, "An algorithm for optimizing the packet size used in wireless ARQ protocols," *Wireless Networks*, vol. 5, no. 4, pp. 279-286, July 1999.

[7] B. Liang and Z. Haas, "Predictive distance-based mobility management for PCS networks," in *Proc. the Joint Conference of the IEEE Computer and Communications Societies (INFOCOM)*, Mar. 1999.

[8] A. Gelb, *Applied Optimal Estimation.* M.I.T. Press, 1974.

[9] T. Camp, J. Boleng and V. Davies, "A survey of mobility models for ad hoc network research," *Wireless Communications & Mobile Computing (WCMC): Special issue on Mobile Ad Hoc Networking: Research, Trends and Applications*, vol. 2, no. 5, pp. 483–502, 2002.

[10] D. Bertsekas and R. Gallager, *Data networks*, Englewood Cliffs, NJ: Prentice-Hall, 1987.

[11] G. Bianchi, “Performance analysis of the IEEE 802.11 distributed coordination function,” *IEEE Journal on Selected Areas in Communications*, vol. 18. no. 3, Mar. 2000.

[12] Qualnet simulator. http://www.qualnet.com/

[13] P. Gupta and P. R. Kumar. “The Capacity of Wireless Networks,” *IEEE Transactions on Information Theory*, vol. 46, no. 2, Mar. 2000.

[14] P802.11, “IEEE standard for wireless LAN medium access control (MAC) and physical layer (PHY) specifications,” Nov. 1997.

[15] C. R. Dow, P. J. Lin, S. C. Chen, J. H. Lin and S. F. Hwang, “A Study of Recent Research Trends and Experimental Guidelines in Mobile Ad Hoc Networks,” in *Proc. the 19th International Conference on Advanced Information Networking and Applications*, vol. 1, pp. 72-77, Mar. 2005.

[16] S. Xu and T. Saadawi, “Does the IEEE 802.11 MAC protocol work well in multihop wireless ad hoc networks?,” *IEEE Commun. Mag.*, vol. 39, pp. 130-137, June 2001.

[17] B. Kwak and N. Song, “A Standard Measure of Mobility for Evaluating Mobile Ad-Hoc Network Performance,” *IEICE Trans. Commun.*, vol. E86-B, n. 11, Nov. 2003.

[18] T. S. Rappaport, *Wireless communications: principles and practice*. Prentice-Hall, 2002.

[19] S. Lin and D. J. Costello, Jr., *Error control coding*. Englewood Cliffs, NJ: Prentice-Hall, 1983.

Appendix

Mathematical Derivation

1. Proof of (2-8)

Let $f_D(D_{nj})$ be the PDF of the link distance from node *n* to node *j*. Then the mean interference can be written

$$I_0 = E\left[\overline{P}\sum_{\substack{n\in G(t)\\ n\neq i}} D_{nj}(t)^{-\alpha}\right] \tag{A-1}$$

$$= \overline{P}\sum_{\substack{n\in G(t)\\ n\neq i}} E\left[D_{nj}(t)^{-\alpha}\right]$$

$$= \overline{P}\sum_{\substack{n\in G(t)\\ n\neq i}}\left[\int_0^{\infty} D_{nj}{}^{-\alpha} f_D(D_{nj})dD_{nj}\right].$$

All nodes in the network are assumed i.i.d. and that have the same mobility pattern. Then the link distance (D_{ij}) of all nodes are also i.i.d such that the PDF of all link distance are same.

$$f_D(D_{nj}) = f_D(D_{ij}). \tag{A-2}$$

The source node *i* is a member of transmission group at time *t*. Therefore, the mean interference can be written as

$$I_0 = \bar{P}(N_G - 1)\int_0^{\infty} D_{ij}^{-\alpha} f_D(D_{ij}) dD_{ij} \ . \tag{A-3}$$

2. Proof of (2-11)

When $D_{ij}(t) = r$, the mean received power at node *j* is

$$E\left[\sum_{n=1}^{N} S(D_{nj}(t))\right] = \bar{P} r^{-\alpha} + E\left[\sum_{\substack{n \in G(t) \\ n \neq i}} \bar{P} D_{nj}(t)^{-\alpha}\right]. \tag{A-4}$$

From (A-4) the inequality (2-10) is

$$\begin{aligned} &\rho N_0 W + \bar{P} r^{-\alpha} + E\left[\sum_{\substack{n \in G(t) \\ n \neq i}} \bar{P} D_{nj}(t)^{-\alpha}\right] \geq P_{sen} \\ &\rho N_0 W + \bar{P} r^{-\alpha} + I_0 \geq P_{sen} \\ &r^{-\alpha} \geq \frac{P_{sen} - \rho N_0 W - I_0}{\bar{P}} \end{aligned} \tag{A-5}$$

where $r^{-\alpha}$ is non-negative value. Therefore if $P_{sen} \geq (\rho N_0 W + I_0)$,

$$r \leq \left[\frac{\bar{P}}{P_{sen} - \rho N_0 W - I_0}\right]^{\frac{1}{\alpha}}. \tag{A-6}$$

If $P_{sen} < (\rho N_0 W + I_0)$,

$$r \leq \infty \tag{A-7}$$

Let R_{sen} be the mean carrier sensing range. The mean carrier sensing range is the maximum value of r so

$$R_{sen} = \begin{cases} \left[\dfrac{\overline{P}}{P_{sen} - \rho N_0 W - I_0} \right]^{\frac{1}{\alpha}}, & P_{sen} \geq \left(I_0 + \rho N_0 W \right) \\ \infty \qquad\qquad , & P_{sen} < \left(I_0 + \rho N_0 W \right). \end{cases} \tag{A-8}$$

3. Proof of (2-13)

When $D_{ij}(t) = r$, the mean SINR at node *j* becomes

$$E\left[\frac{\overline{\mathrm{P}}\, r^{-\alpha}}{\rho N_0 W + \overline{P} \sum_{\substack{n \in G(t) \\ n \neq i}} D_{nj}(t)} \right] = \frac{\overline{P} r^{-\alpha}}{\rho N_0 W + I_0}. \tag{A-9}$$

From (A-7) the inequality (2-12) can be extended to

$$\begin{aligned} & \frac{\overline{P} r^{-\alpha}}{\rho N_0 W + I_0} \geq \gamma_{\min} \\ & r^{-\alpha} \geq \frac{\gamma_{\min} \left(\rho N_0 W + I_0 \right)}{\overline{P}} \\ & r \leq \left[\frac{\gamma_{\min} \left(\rho N_0 W + I_0 \right)}{\overline{P}} \right]^{\frac{1}{\alpha}}. \end{aligned} \tag{A-10}$$

Let $R_{\max}$ be the maximum average communication range. The maximum average communication range is the maximum value of r, therefore we obtain,

$$R_{\max} = \left[\frac{\overline{P}}{\gamma_{\min}\left(\rho N_0 W + I_0\right)} \right]^{\frac{1}{\alpha}}. \tag{A-11}$$

4. Proof of (5-11)

The CDF of the mean SINR is defined as

$$F_{\Gamma}(\gamma) = P\left\{ E\left[X(D) \right] \le \gamma \right\}. \tag{A-12}$$

From (5-9) the CDF of the mean SINR can be represented as

$$\begin{aligned} F_{\Gamma}(\gamma) &= P\left\{ \frac{\overline{P} D^{-\alpha}}{\rho N_0 W + I_0} \le \gamma \right\} \\ &= P\left\{ D \ge \left(\frac{\overline{P}}{\gamma\left(\rho N_0 W + I_0\right)} \right)^{\frac{1}{\alpha}} \right\} \\ &= 1 - P\left\{ D \le \left(\frac{\overline{P}}{\gamma\left(\rho N_0 W + I_0\right)} \right)^{\frac{1}{\alpha}} \right\} \\ &= 1 - F_D\left(\left(\frac{\overline{P}}{\gamma\left(\rho N_0 W + I_0\right)} \right)^{\frac{1}{\alpha}} \right) \end{aligned} \tag{A-13}$$

Therefore, form (5-7) the CDF of the mean SINR is expressed in terms of a Beta CDF as

$$F_{\Gamma}(\gamma) = 1 - F_{beta}\left(\frac{1}{2R + r_0} \left[\frac{\overline{P}}{\left(\rho N_0 W + I_0\right)} \right]^{\frac{1}{\alpha}} \left(\frac{1}{\gamma} \right)^{\frac{1}{\alpha}} \right). \tag{A-14}$$

5. Proof of (5-14)

The PDF of the mean SINR can be defined from

$$f_{\Gamma}(\gamma)=\frac{\partial F_{\Gamma}(\gamma)}{\partial \gamma}. \tag{A-15}$$

From (5-12) the PDF of mean SINR is obtained from

$$\begin{aligned}
&\frac{\partial F_{\Gamma}(\gamma)}{\partial \gamma}=\frac{\partial\left(1-F_{beta}\left(Z_{\Gamma}(\gamma)\right)\right)}{\partial \gamma} \\
&=-\frac{Z_{\Gamma}(\gamma)}{\partial \gamma} f_{beta}\left(Z_{\Gamma}(\gamma)\right) \\
&=-\frac{\frac{1}{2R+r_0}\left[\frac{\overline{P}}{\left(\rho N_0 W+I_0\right)}\right]^{\frac{1}{\alpha}}\left(\frac{1}{\gamma}\right)^{\frac{1}{\alpha}}}{\partial \gamma} f_{beta}\left(Z_{\Gamma}(\gamma)\right) \\
&=\frac{1}{2R+r_0}\left[\frac{\overline{P}}{\left(\rho N_0 W+I_0\right)}\right]^{\frac{1}{\alpha}}\left(\frac{1}{\gamma}\right)^{\frac{1}{\alpha}+1}\frac{1}{\alpha} f_{beta}\left(Z_{\Gamma}(\gamma)\right) \\
&=\frac{1}{2R+r_0}\left[\frac{\overline{P}}{\left(\rho N_0 W+I_0\right)}\right]^{\frac{1}{\alpha}}\left(\frac{1}{\gamma}\right)^{\frac{1}{\alpha}}\frac{1}{\alpha\gamma} f_{beta}\left(Z_{\Gamma}(\gamma)\right) \\
&=\frac{Z_{\Gamma}(\gamma)}{\alpha\gamma} f_{beta}\left(Z_{\Gamma}(\gamma)\right).
\end{aligned} \tag{A-16}$$

Therefore, the PDF of the mean SINR becomes

$$f_{\Gamma}(\gamma)=\frac{Z_{\Gamma}(\gamma)}{\alpha\gamma} f_{beta}\left(Z_{\Gamma}(\gamma)\right). \tag{A-17}$$

6. Proof of (5-17)

The CDF of the mean BER is defined as

$$F_{\mathrm{B}}(p) = P[\mathrm{B} \le p]. \tag{A-18}$$

From (5-15) and (A-12) the CDF of the mean BER is

$$\begin{aligned} P[\mathrm{B} \le p] &= P\left[E\left[X(D)\right] \ge H^{(-1)}(p)\right] \\ &= 1 - P\left[E\left[X(D)\right] \le H^{(-1)}(p)\right] \\ &= 1 - F_{\Gamma}\left(\left(\frac{a}{p}\right)^{\frac{1}{\alpha b}}\right). \end{aligned} \tag{A-19}$$

Therefore, from (5-12) the CDF of the mean BER can be written as

$$\begin{aligned} F_{\mathrm{B}}(p) &= 1 - \left(1 - F_{beta}\left(Z_{\Gamma}\left(\left(\frac{a}{p}\right)^{\frac{1}{\alpha b}}\right)\right)\right) \\ &= F_{beta}\left(\frac{1}{2R + r_0}\left[\frac{\bar{P}}{(\rho N_0 W + I_0)}\right]\left(\frac{a}{p}\right)^{\frac{1}{\alpha b}}\right). \end{aligned} \tag{A-20}$$

7. Proof of (5-20)

The PDF of the mean BER is defined as

$$f_{\mathrm{B}}(p)=\frac{\partial F_{\mathrm{B}}(p)}{\partial p}. \tag{A-21}$$

From (5-18) the PDF of the mean BER can be represented as

$$\begin{aligned}
\frac{\partial F_{\mathrm{B}}(p)}{\partial p} &= \frac{\partial F_{beta}\left(\mathrm{Z}_{\mathrm{B}}(p)\right)}{\partial p} \\
&= \frac{\partial\left(\frac{1}{2R+r_0}\left[\frac{\overline{P}}{\left(\rho N_0 W+I_0\right)}\right]\left(\frac{a}{p}\right)^{\frac{1}{\alpha b}}\right)}{\partial p} f_{beta}\left(\mathrm{Z}_{\mathrm{B}}(p)\right) \\
&= -\frac{1}{\alpha b p}\left(\frac{1}{2R+r_0}\left[\frac{\overline{P}}{\left(\rho N_0 W+I_0\right)}\right]\left(\frac{a}{p}\right)^{\frac{1}{\alpha b}}\right) f_{beta}\left(\mathrm{Z}_{\mathrm{B}}(p)\right) \\
&= \frac{\mathrm{Z}_{\mathrm{B}}(p)}{\alpha b p} f_{beta}\left(\mathrm{Z}_{\mathrm{B}}(p)\right).
\end{aligned} \tag{A-22}$$

VITA

Dong Chul Go

Candidate for the Degree of

Master of Science

Thesis: AN ALGORITHM FOR OPTIMIZING PACKET SIZE IN MOBILE AD HOC NETWORKS

Major Field: Electrical Engineering

Biographical:

Personal Data: Born in Teagu city, S. Korea, on September 26, 1970.

Education: Graduated from Hyunpung High School, Taegu, S. Korea in March 1989; received Bachelor of Science degree in Electrical engineering from Korea Air Force Academy (KAFA) in March 1993; In July of 2005, received Master of Science degree in electrical engineering from the Oklahoma State University, U.S.A.

Experience: Raised in Taegu city until high school; promoted as an Air Force officer after graduation of KAFA; have worked as a fight pilot and a flight instructor in the Korean Air Force, from 1993 to present; Currently ranked as Major of the Air Force of the Republic of Korea; From August of 2003 to July of 2005 worked as a Research Assistant in the Advanced Communication Systems Engineering Laboratory (ACSEL) and the Oklahoma Communication Laboratory for Networking & Bioengineering (OCLNB) of the Oklahoma State University.

Professional Memberships: IEEE Student Member, OSU Chapter, 2003.

Name: Dong Chul Go Date of Degree: July 2005

Institution: Oklahoma State University Location: Stillwater, Oklahoma

Title of Study: AN ALGORITHM FOR OPTIMIZING PACKET SIZE IN MOBILE AD HOC NETWORKS

Pages in Study: 67 Candidate for the Degree of Master of Science

Major Field: Electrical Engineering

Scope and Method of Study: This thesis proposes an algorithm to optimize packet size in mobile ad hoc networks (MANET). In this thesis, the packet size is adapted to maximize the communication performance through the automatic repeat request (ARQ) protocol. The optimal packet size is chosen by an algorithm based on the estimation of the channel from the number of retransmission requests and the link statistics obtained from the mobility pattern. By adapting the non-uniform distribution of the bit error rate (BER) obtained from the mobility pattern analysis, it is possible to estimate channel conditions more accurately from the number of retransmission requests and to improve the system performance.

Findings and Conclusions: It was found that the distribution of the link distance among mobile nodes following the Gauss-Markov mobility pattern in a circularly shaped area well fits the Beta distribution function. From the simulation results it is observed that when the interference increases, or the path loss exponent increases, or when the size of history decreases, the throughput and efficiency performance will decrease. Based on an analysis in various wireless environments, the algorithm proposed in this thesis shows almost an optimal throughput efficiency performance, and it gives better performance than the algorithm in [6], which uses an uniform distribution function for the estimation of the channel condition. By adapting the Beta distribution of the BER obtained from the mobility pattern, it is possible to estimate the channel conditions more accurately from the number of retransmission requests and to improve the throughput and utilization performance of MANET communication systems.

ADVISER'S APPROVAL: Jong-Moon Chung